



STUDY OF THE GROWTH PARAMETERS INVOLVED IN SYNTHESIZING BORON CARBIDE FILAMENTS

FINAL REPORT

by

A. Gatti , E. Feingold, J. J. Gebhardt, J. Berry , V. A. Cordua

prepared for

NATIONAL AERONAUTICS AND SPACE ADMINISTRATION

contract NASw-1383

FACILITY FORM 602

N 67 191 32 (ACCESSION NUMBER)	(THRU)
52 (PAGES)	1 (CODE)
CR-82447 (NASA CR OR TMX OR AD NUMBER)	17 (CATEGORY)

SPACE SCIENCES LABORATORY

GENERAL  ELECTRIC

MISSILE AND SPACE DIVISION

FINAL REPORT

STUDY OF THE GROWTH PARAMETERS INVOLVED
IN SYNTHESIZING BORON CARBIDE FILAMENTS

by

A. Gatti, E. Feingold, J. J. Gebhardt, J. M. Berry, V. A. Cordua

prepared for

NATIONAL AERONAUTICS AND SPACE ADMINISTRATION

November 1966

CONTRACT NASw-1383

U67 19132

Space Sciences Laboratory
GENERAL ELECTRIC COMPANY
Missile and Space Division

TABLE OF CONTENTS

<u>Section</u>	<u>Page</u>
Summary	v
I. Introduction	1
II. Experimental Procedures and Results	3
A. Growth Studies	3
1. Direct Evaporation Process	3
2. Chemical Vapor Deposition (CVD) Process	5
B. Whisker Annealing Studies	15
C. Whisker Characterization	21
1. Evaluation of Curved Whiskers	21
2. Evaluation of Annealed Whiskers	27
III. Composite Studies	31
A. Aluminum - B_4C Whisker Composites	31
B. Aluminum - B_4C/W Filament Composites	33
IV. Discussion & Conclusions	43
References	46
Acknowledgements	47

ILLUSTRATIONS

<u>Figure</u>	<u>Page</u>
1. Schematic Diagrams Showing the Evolution of the Direct Vapor Process for Growing B_4C Whiskers	4
2. Photograph (about 1/10th size) of Resistance Heated Graphite Furnace	7
3. Schematic Flow Diagram of B_4C Deposition System	8
4. Sketch of B_4C Deposition Zones in Deposition Chamber	12
5. Typical Views of B_4C Deposition Products Formed by the Chemical Vapor Deposition Process A. Debris - 230X, B. Typical Whiskers - 115X C. Same as B at 230X	13
6. Schematic Drawing of Graphite Chamber for Annealing B_4C Whiskers	16
7. Examples of Curved B_4C Whiskers as They Appear A. Before Annealing - 30X B. After Annealing - 30X	17
8. Example of Whisker Surface of an Annealed Whisker - 300X	18
9. The Effect of Annealing Temperature on the Room Temperature Tensile Strength of B_4C Whiskers	20
10. Hexagonal Unit Cell Lattice Parameters a and c for Curved and Straight Portions of a Single B_4C Whisker	23
11. Sketch of a Curved B_4C Whisker	24
12. Spring Analog of Internal Stresses in a Curved B_4C Whisker	26
13. B_4C Whiskers Before and After Annealing for 1 Hour at $1900^\circ C$ and 85×10^{-3} Torr - 1300X	28
14. Schematic Representation of Annealed B_4C Whiskers Showing Roughened (0k0) Planes and Resulting Edge Notches	30

ILLUSTRATIONS (Cont'd)

<u>Figure</u>		<u>Page</u>
15.	Resume of Possible Factors Which Affect the Strength of Composite Materials Reinforced by Discontinuous Filaments	35
16.	Schematic Diagram Outlining the Hot Pressing Procedure for Producing B ₄ C/W-Aluminum Composites	36
17.	Sketch Showing Processing Details to Produce B ₄ C/W-Aluminum Composites for Estimating Values of the Filament Critical Length, L _c	39
18.	Broken Sections of B ₄ C/W Filaments Retrieved from Hot Pressed Aluminum Composites (17X)	40
19.	Typical Tensile Fractures of B ₄ C/W Filaments in Hot Pressed Aluminum Composite (593X)	41

STUDY OF THE GROWTH PARAMETERS INVOLVED IN SYNTHESIZING BORON CARBIDE FILAMENTS

by

A. Gatti, E. Feingold, J. J. Gebhardt, J. M. Berry, V. A. Cordua

General Electric Company

SUMMARY

The purpose of this program has been 1) to investigate the parameters leading to the growth of B_4C whiskers, 2) to characterize the B_4C whiskers in terms of their mechanical properties and crystalline perfection, and 3) to investigate the factors affecting the efficient transfer of stresses from the matrix to the whiskers.

Whiskers of B_4C were grown in a chimney-type graphite resistance furnace. The temperature gradient developed at the chimney top was used to control the supersaturation of B_4C vapor during nucleation and growth of the whiskers. However, the geometry of the whisker growth zone in this furnace resulted in curved whiskers instead of the more desirable straight variety. Thus, studies of the growth and deposition-zone geometry on whisker production were conducted. A new furnace geometry resulted from these studies, and has resulted in producing a much larger number of whiskers per run. However, these whiskers were not as long as the whiskers grown previously. Efforts are continuing to grow longer whiskers.

Other studies were directed towards producing B_4C whiskers by a chemical vapor deposition method which would be more amenable to economic scale-up of the growth process. Kinetic and thermodynamic calculations were re-examined and B_4C whiskers have been grown utilizing boron tribromide and carbon tetrachloride at temperatures near $1400^\circ C$.

Heat treatment of the curved whiskers was investigated. At annealing temperatures above $1500^\circ C$, the whiskers were found to straighten. Some crystallographic surfaces of these whiskers were roughened, however, thus increasing the probability of having weakening notches. All whiskers annealed at $1600^\circ C$ and above became straighter but did not retain their as-grown strength.

X-ray studies of a curved whisker showed that regions with internal stresses on the order of $E^*/600$ (ca. $\sim 100,000$ psi) exist thus further emphasizing that curvature must be minimized in whiskers which are to be used in composites.

Aluminum- B_4C whisker composites were produced by vacuum infiltration. From a fabrication point of view, the composites were free of voids and appeared sound. The room temperature tensile strength values of these composites averaged 10,500 psi.

A number of aluminum- B_4C continuous filament composites (the filaments were made by vapor depositing B_4C on a boron-tungsten filament) were also produced by vacuum infiltration using the same techniques developed for the whisker composites. The composites reinforced with the continuous filaments utilized 90% or more of the strength of the filaments, based on the rule of mixture calculations. Composite strengths as high as 86,000 psi were observed. However, for composites reinforced with discontinuous filaments only about 70% of the theoretical strength was attained.

A substitute system based on the B_4C/W filament material appears to be a satisfactory means for investigating the strengthening characteristics and the mechanical behavior of materials reinforced with short B_4C filaments. The factors affecting the transfer of stresses from a ductile matrix (aluminum) to short brittle filaments (B_4C/W) can be studied during the period in which the problems of B_4C whisker supply, B_4C whisker length, and B_4C whisker curvature are being solved.

To further utilize this approach, a hot pressing technique has been developed for producing composite specimens in which the geometric variables can be controlled with reasonable precision. Thus variables such as critical fiber length, fiber spacing and fiber overlap can be studied with greater precision than has been possible in the past.

* Where E is the elastic modulus

I. INTRODUCTION

Boron carbide whiskers exhibit properties which make them attractive candidates for utilization in composite materials. In terms of their high strength, high elastic modulus and low density, these whiskers, when used as reinforcements, offer a great potential for high strength-to-weight and high stiffness-to-weight materials for space applications. In addition, their refractory properties make them valuable for high temperature applications.

During the past three years, a program^(1,2) was undertaken 1) to study the parameters leading to the growth of B_4C whiskers, 2) to characterize the B_4C whiskers in terms of their mechanical properties and crystalline structure, and 3) to investigate their reinforcing potential in several matrices. Although more than one method for growing B_4C whiskers was investigated, the most successful one was the direct evaporation method. It consists of vaporizing B_4C powder at high temperatures and subsequently condensing B_4C whiskers on a graphite substrate at lower temperatures.⁽¹⁾ It was also shown that a 'catalyst' (vanadium) was essential for growth to proceed at reasonable rates. This method, in conjunction with the vanadium addition to the initial B_4C powder, was used to study the growth parameters and to obtain an adequate supply for whisker characterization and for composite studies.

Tensile tests of the whiskers were performed, and a wide range of values were recorded; from about 200,000 psi to 2,000,000 psi. It was found⁽²⁾ that the strength of the whiskers (based on about 30 tests) did not vary with whisker size, nor did the whiskers show a significant loss in strength at test temperatures up to 1000°C. Most of the whiskers, when observed under the microscope exhibited growth steps on their surfaces, and only the strongest whiskers were essentially free of these steps. Most of the whiskers were also observed to have their growth axis parallel to the $\langle 100 \rangle$ crystallographic direction of the hexagonal cell; viz., parallel to the \vec{a} unit cell edge. Composites of an epoxy resin and of

pure aluminum reinforced with the B_4C whiskers were prepared. Although the volume fractions of the whiskers was low (about 5%), tensile strengths as high as 29,000 psi were recorded.

During the course of the growth study, improvements in furnace geometry led to increased whisker yields. However, it was apparent that the direct vaporization process was not amenable to scale-up because of an inherently low whisker growth rate and because of the high ($1900^{\circ}C$) temperatures involved. Therefore, a renewed look at the chemical vapor deposition (CVD) method was undertaken. This final report, which covers the period from February 1966 to November 1966, includes the results of recent studies on the CVD process, on the annealing of curved whiskers grown by the direct evaporation process, and on factors affecting the transfer of stresses from the matrix to the reinforcing whiskers.

II. EXPERIMENTAL PROCEDURES AND RESULTS

A. GROWTH STUDIES

Several possible methods for growing B_4C whiskers were investigated and evaluated^(1,2). These methods were based on either the 1) direct evaporation and condensation of B_4C , or 2) the production of B and C vapor species and their subsequent reaction and condensation as B_4C whiskers (previously called the dynamic method). These two methods will be discussed.

1. Direct Evaporation Process

This process consists essentially of vaporizing B_4C powder at high temperatures ($1900^\circ C$) and condensing the vapor in a cooler chamber (at about $1700^\circ C$). In all cases, graphite was used for the chamber walls. Several chamber configurations were investigated, and these are shown schematically in Figure 1.

The first chamber configuration is shown in Figure 1A. Finely divided powder of B_4C is spread out on a 'lazy-Susan' tray which is heated in vacuo ($\sim 50\mu$) at $1900^\circ C$. The resulting vapor is carried upwards into a cooler chamber, where it condenses on the chamber walls as B_4C whiskers. The geometric configuration of the whisker deposition chamber was found to be a major variable affecting the nucleation and growth of the whiskers. An internal mandrel (Figure 1B) was next inserted into the growth chamber in order to increase the surface area over which nucleation and growth could occur. This configuration, coupled with the use of a catalyst (vanadium) which was mixed with the starting B_4C powder,⁽¹⁾ led to a substantial increase in the yield of fine B_4C whiskers. The use of the mandrel also resulted in symmetrical temperature gradients within the growth chamber⁽²⁾. However, the chief drawback of this growth system was that most of the whiskers were curved, due to residual stresses within the whiskers. These stresses resulted from the non linear thermal and compositional gradients in the vapor surrounding the deposition surface. A growth mechanism was postulated which would explain the curved nature of the whiskers⁽⁸⁾.

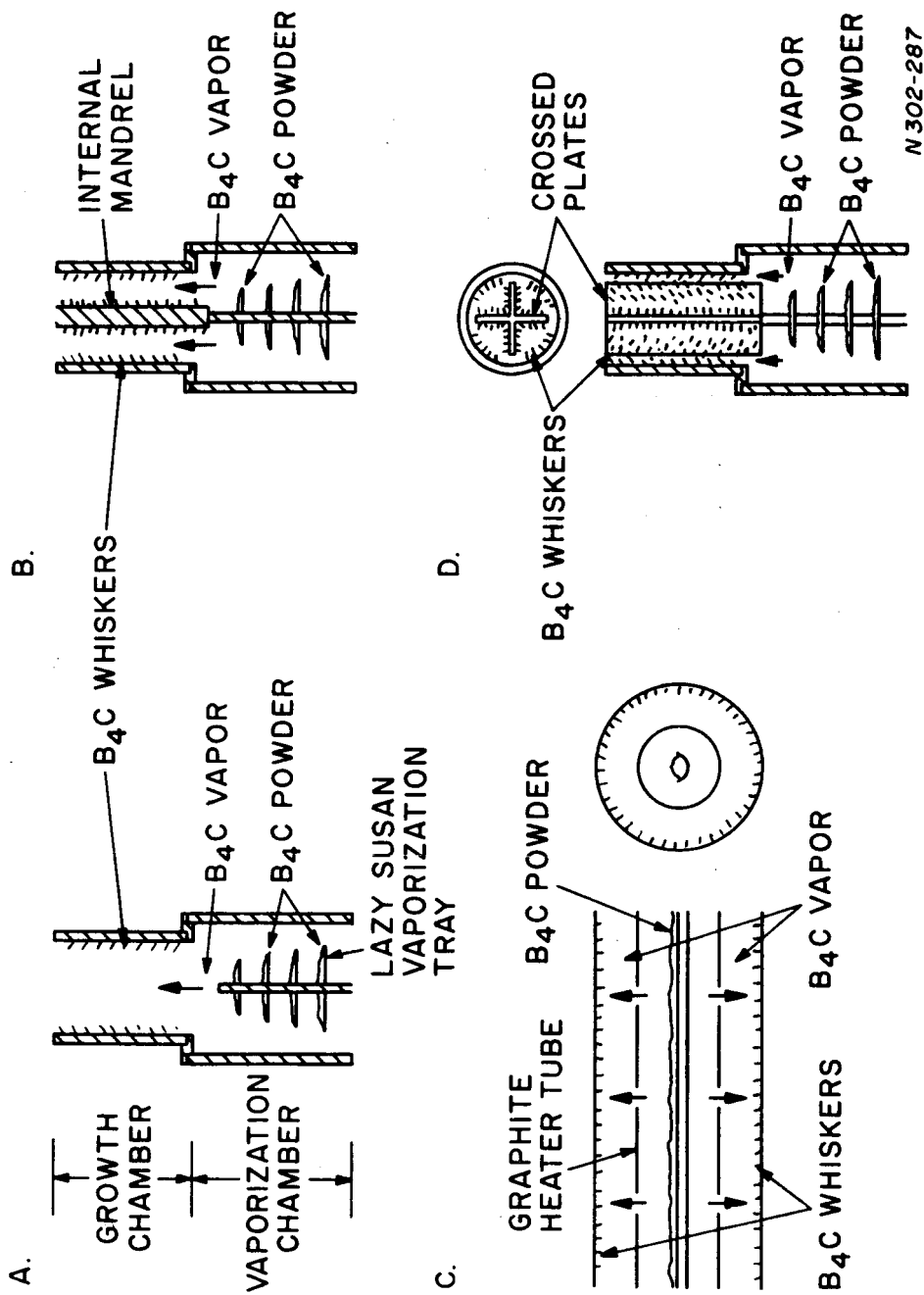


Figure 1. Schematic Diagrams Showing the Evolution of the Direct Vapor Process for Growing B_4C Whiskers

- A. First design: Vaporization-Condensation Chambers
- B. Internal Mandrel Design
- C. Radial Furnace Design
- D. Crossed-Graphite Plate Design

In order to remedy the curved growth, a new furnace geometry was utilized⁽²⁾. This consisted of a central tube containing the heated B_4C powder (Figure 1C), so that both the B/C vapor and the temperature gradients emanated radially from the heater tube to a concentrically located condensation surface. The use of this radial furnace design increased the deposition surface by several orders of magnitude over the previous configurations (Figures 1A and B). Although whiskers were grown, their sizes were not greater than those produced previously. Also, this configuration did not permit adequate control over the thermal gradients, which is necessary to optimize whisker growth conditions.

As a result of the previous growth chamber configuration studies, another modification was developed (Figure 1D), which had a twenty-fold increase in deposition surface area over the configurations shown in Figures 1A and B. In addition, the use of the crossed-graphite plates resulted in approximately an order of magnitude increase in the number of whiskers grown per run. An added result of this geometric change has been the reduction of the number of curved whiskers grown, presumably due to the alteration of the symmetrically shaped temperature gradients which were present in the former deposition geometry. However, even these encouraging results have neither increased the whisker yield sufficiently nor simplified the growth process so that a large scale-up would be feasible. Thus, although as has been pointed out already, the evaporative method for the preparation of boron carbide whiskers is a relatively convenient way of obtaining research quantities of materials, the yield per unit operating time and unit power input is low and the total production is insufficient for fully investigating the important areas of whisker coating and composite fabrication.

2. Chemical Vapor Deposition (CVD) Process

In view of the need for an improved whisker growth process, interest was renewed in processes investigated earlier in this program,⁽¹⁾ but set aside in favor of the evaporation method suitable for acquiring whiskers for characterization. In the interim, vapor phase work on other programs⁽³⁾

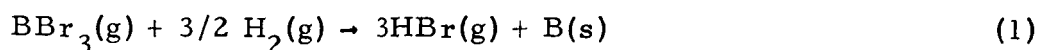
had added to the background of experience available and this was applied to the dynamic vapor processes for producing B_4C whiskers. Accordingly, an apparatus was assembled to permit passage of reactive gases containing boron and carbon onto a heated tube under controlled conditions.

Several factors contribute to the yield and type of whiskers which can be grown from a particular vapor system. These include the thermodynamics and kinetics of the production of reduced species in the vapor phase, concentration and gas velocity, geometry, temperature and total pressure, and the nature of the substrate. Temperature is also a primary factor in the kinetics of the whisker growth, as differentiated from the kinetics of reduced specie formation. A proper balance must be sought between the amount of energy supplied to promote reduced specie formation and the required amount for surface and bulk diffusion in the whisker itself. If too much energy is supplied the deposition rate will be too fast relative to the diffusion rate, and overgrowths, such as sooty and polycrystalline deposits, will result. If on the other hand, too little energy is supplied, fewer nuclei form, the deposition rate falls off considerably and the whisker production rates suffer.

As a starting point, $1400^{\circ}C$ was taken as a deposition temperature at which both boron trichloride and carbon tetrachloride would be completely reduced at equilibrium. The rate of approach to equilibrium must be determined experimentally however.

Figure 2 shows the resistance heated graphite furnace used in carrying out whisker deposition experiments using the chemical vapor deposition method. The primary features are a $1\frac{5}{8}$ " I.D. graphite heating element and a 1" I.D. deposition tube located in the heating element. Figure 3 is a schematic diagram of the gas flow and control system.

The feed materials (boron tribromide and carbon tetrachloride) are both thermodynamically unstable in the presence of hydrogen at $1400^{\circ}C$, which should assure a controllable source of boron and carbon gas phase species. For example, using the reaction



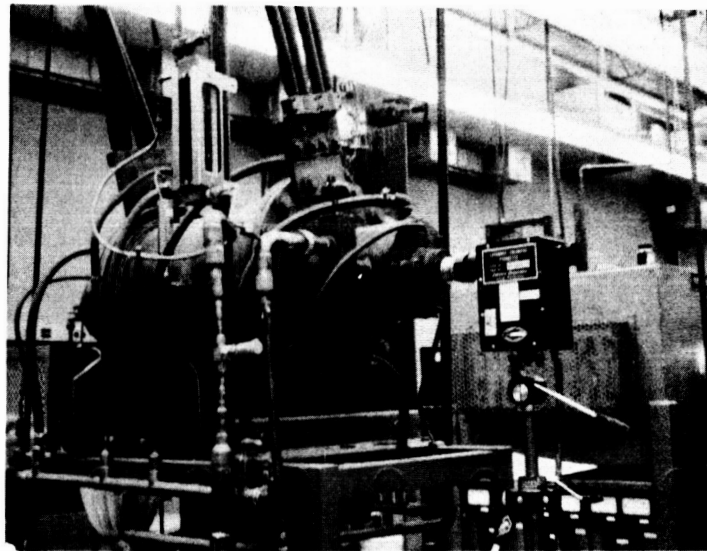


Figure 2. Photograph (about 1/10 th Size) of Resistance Heated Graphite Furnace

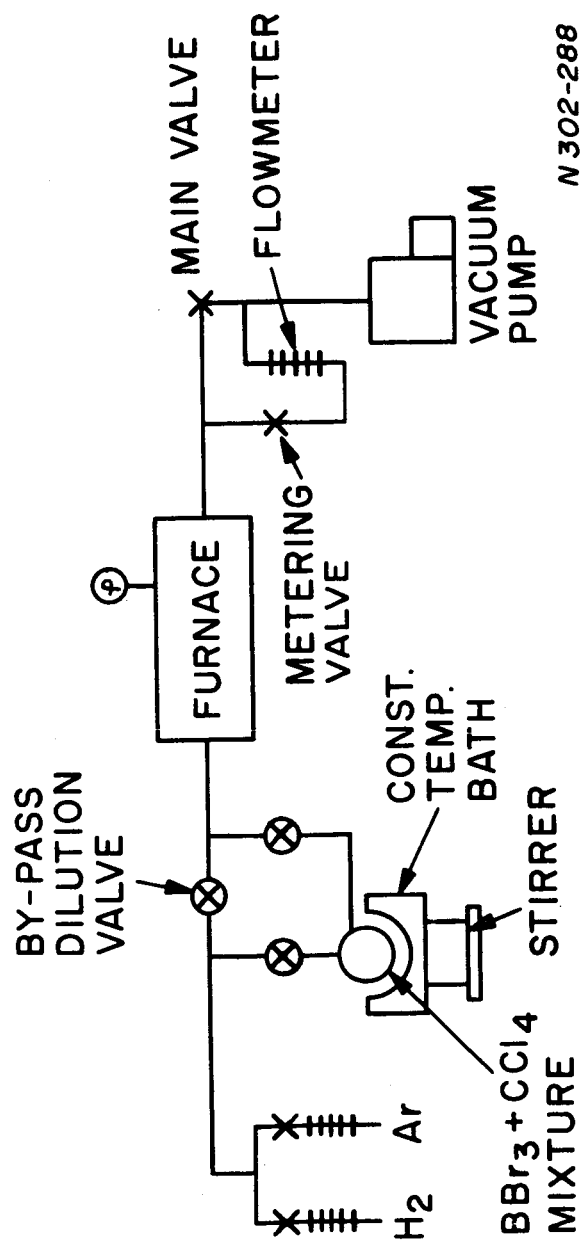


Figure 3. Schematic Flow Diagram of B₄C Dynamic Vapor System

the equilibrium expression can be derived as follows, where y is the fraction converted, R is the ratio of hydrogen to boron tribromide and P is the total pressure.

	Initial	Equilibrium
BBr ₃	1	1-y
H ₂	R	R-3/2 y
HBr	0	<u>3y</u>
Total moles.		1 + R + y/2

The equilibrium constant for the reaction,
$$\frac{(P_{\text{HBr}})^3}{(P_{\text{BBr}_3})(P_{\text{H}_2})^{3/2}}$$

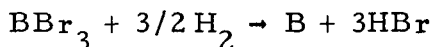
Expressing pressure as mole fraction

$$K = \frac{\left[\frac{3y}{1+R+y/2}\right]^3}{\left[\frac{1-y}{1+R+1/2y}\right] P \left[\frac{R-3/2y}{1+R+1/2y} P\right]^{3/2}} \quad (2)$$

or

$$K = \frac{3^3 y^3 P^{1/2}}{(1-y)(R-3/2y)^{3/2} (1+R+1/2y)^{1/2}} \quad (3)$$

At 1700°K, the value of K may be obtained from the thermodynamic free energies of formation of the components i. e.,



$$-40.79 \qquad 3(-15.47)$$

$$\Delta F = -46.41 + 40.79 = -5.62 \text{ Kcal,}$$

and since $\Delta F = -nRT \ln K$,

$$\log K = 0.716 \text{ and } K = 5.2.$$

Using the equilibrium expression for K (equation 3), and assuming an initial ratio R of hydrogen to boron tribromide of 40 (i. e., $P_{\text{H}_2} = 712 \text{ torr}$
 $P_{\text{BBr}_3} = 18 \text{ torr}$)

$$K = \frac{27 y^3}{(1-y)(40-3/2y)^{3/2} (41+1/2y)^{1/2}} = 5.2$$

By substitution, the value of y is seen to approach unity (>0.99) i.e., conversion is almost complete. A similar calculation gives the same result for carbon tetrachloride at 1700°K . (ca., 1400°C) Inasmuch as the deposition mechanism is not known, it seemed advisable to feed a vapor mixture to the furnace which would yield a stoichiometric ratio of boron and carbon in the gas phase, assuming identical kinetics of reduction for the two materials. From the vapor pressure curves for boron tribromide and carbon tetrachloride, it was calculated as follows that about a 7:1 boron to carbon mole ratio in the liquid phase at 0°C would yield an equilibrium vapor stoichiometry over the liquid of 4:1. At 0°C , $P_{\text{BBr}_3} = 18$ torr and $P_{\text{CCl}_4} = 30$ torr. The total pressure over the liquid mixture, $P_{\text{tot}} = P_{\text{BBr}_3}^{\circ} N_{\text{BBr}_3} + P_{\text{CCl}_4}^{\circ} N_{\text{CCl}_4}$ where P° is the vapor pressure of the pure liquid and N is its mole fraction in the mixture. Converting to moles,

$$P_{\text{BBr}_3} = P_{\text{BBr}_3}^{\circ} \cdot N_{\text{BBr}_3} = P_{\text{BBr}_3}^{\circ} \cdot \frac{m_{\text{BBr}_3}}{(m_{\text{BBr}_3} + m_{\text{CCl}_4})}.$$

Since the pressure of BBr_3 is to be four times that of CCl_4 , one may substitute in this expression as follows using the appropriate pressures at 0°C .

$$18 \cdot \frac{m_{\text{BBr}_3}}{m_{\text{BBr}_3} + m_{\text{CCl}_4}} = 4 \cdot 30 \cdot \frac{m_{\text{CCl}_4}}{m_{\text{BBr}_3} + m_{\text{CCl}_4}}$$

Solving for the respective moles of each component gives the result that a 6.7:1 mole ratio of BBr_3 to CCl_4 in the liquid phase at 0°C will have a 4:1 BBr_3 and CCl_4 mole ratio in the vapor. Such a mixture was made up in a nitrogen purged dry box and placed in the liquid evaporator shown in Figure 3. A stirrer was provided to ensure continued mixing of the liquids so that the surface layer would not be depleted of the more volatile component, CCl_4 .

Hydrogen at one atmosphere was passed through the saturator flask to entrain the halide mixture and carry it into the furnace. The furnace exhaust was connected to a vacuum pump through a micrometer valve so

that gas pressure in the furnace could be maintained at a constant level at any pressure. Initial experiments were conducted at atmospheric pressure. At this pressure, however, the halide components constituted approximately one percent of the total gas feed.

Gas feed rates in the initial experiment were chosen so that the linear gas velocity would be quite low in the one-inch diameter deposition tube. Linear gas velocities used in alumina whisker deposition and in silicon carbide whisker deposition⁽⁷⁾ were taken as the extremes within which initial gas velocities would be set.

The initial run was made using an internal deposition configuration shown in Figure 4A. The deposition tube was split lengthwise to facilitate removal of the product, and the lid was not used. After three hours of deposition at 1400°C the tube was removed and examined. In two regions of the tube, evidence of a concentrated zone of reaction products was obvious. Crystalline and dendritic growths of boron carbide were noted as well as numerous overgrown whiskers. Whiskers were also observed on the heating element, and on the outside diameter of the deposition tube. The two concentrated areas of deposition are traceable to the gas pattern within the deposition zone. Gas enters through the nozzle as shown in Figure 4B at a relatively high velocity, and slows down inside the tube due to the increase in diameter. Gas phase reactions occur and build up a supersaturation of boron and carbon species which reach a critical point and condense. Further along the tube, the gas goes through another constriction in the connector plug, and the process is repeated in the second chamber in the tube.

X-ray analysis of both the whiskers and the solid deposit showed it all to be crystalline boron carbide. Figures 5A and B are typical views of the product, and in particular, Figure 5C shows the marked resemblance between boron carbide whiskers grown by the chemical vapor deposition process and those grown by the direct vapor process. Numerous overgrowth areas indicate that the degree of supersaturation was somewhat high, and further experiments were undertaken with a more dilute gas, obtained by partially by-passing the hydrogen flow through the saturator.

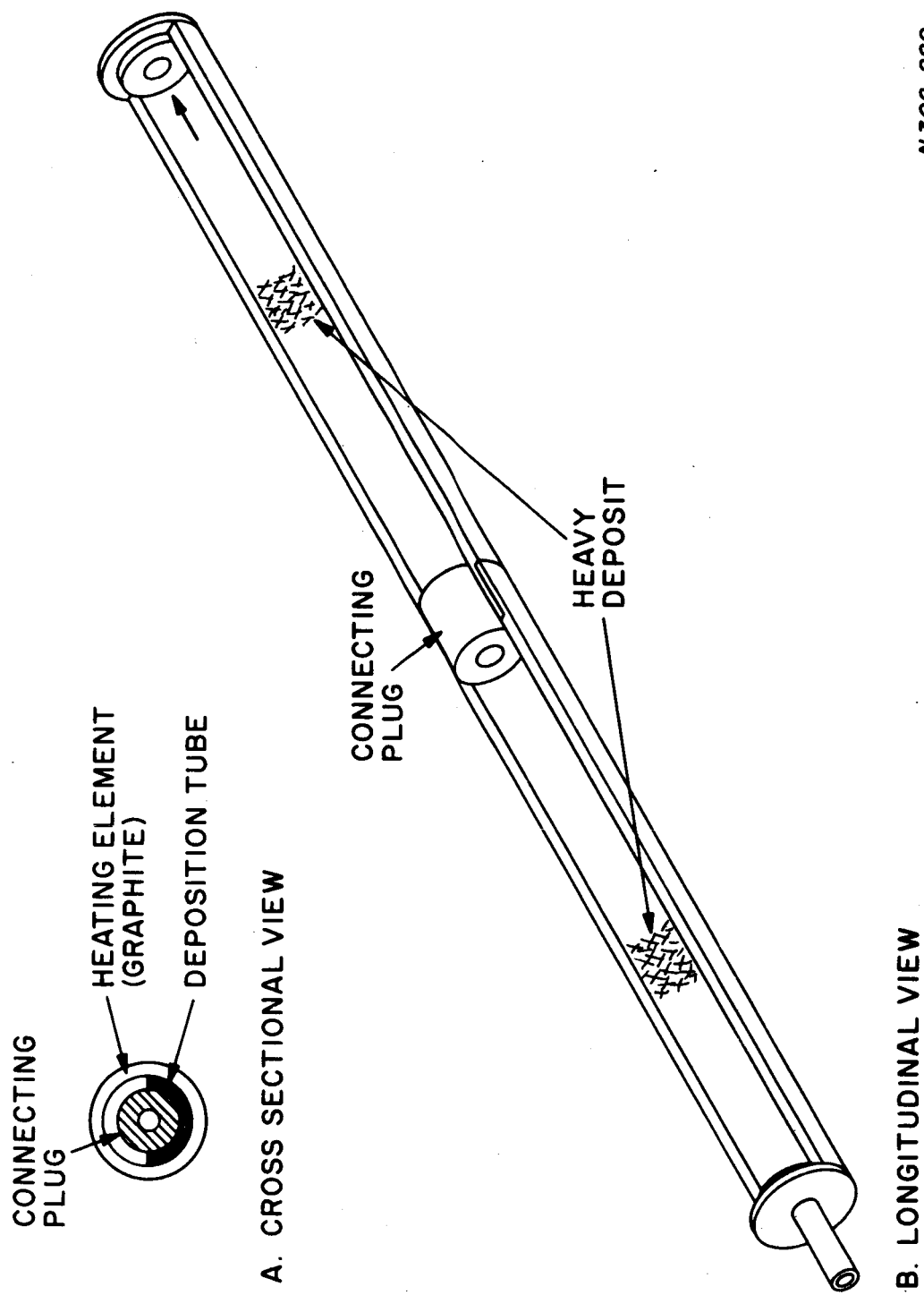
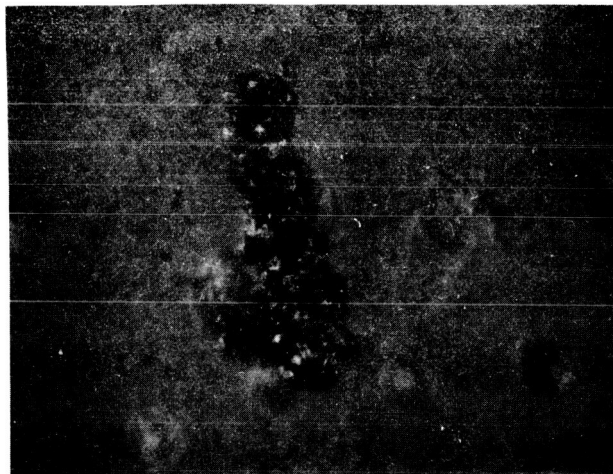
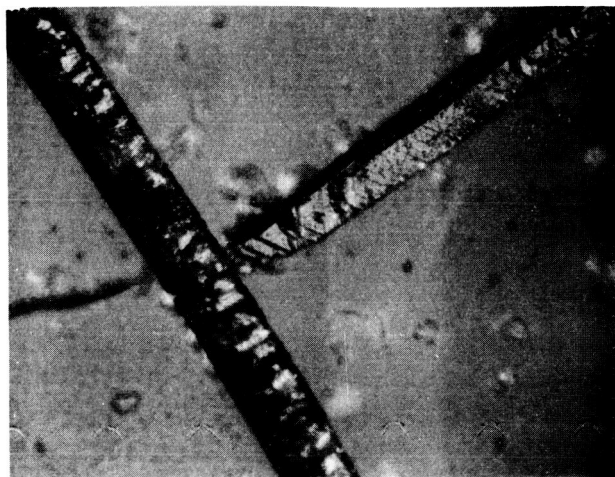


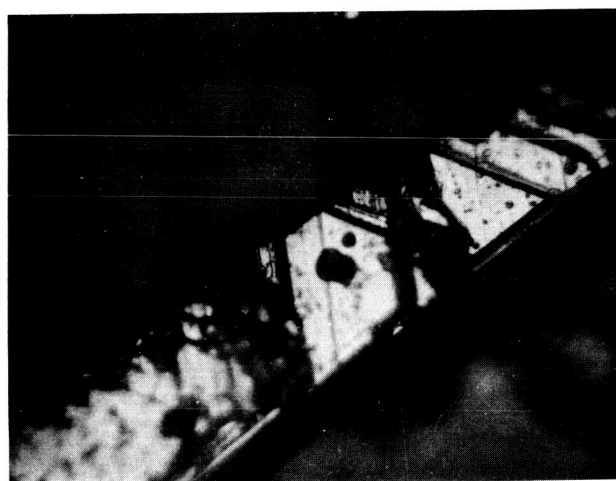
Figure 4. Sketch of B_4C Deposition Zones in Deposition Chamber



A



B



C

Figure 5. Typical Views of B_4C Deposition Products Formed by the Chemical Vapor Deposition Process

- A. Debris - 230X
- B. Typical Whiskers - 115X
- C. Same as B but at 230X

Gas sampling ports (silicone rubber diaphragms) were installed before and after the furnace for analysis of feed and spent gases. However, after several runs with no success in growing whiskers, it was deduced that these ports were a source of leakage. Because of the very small amount of easily hydrolyzed boron halide in the feed stream, it took several runs for sufficient oxide to build up to identify the problem. In each of these runs, the formation of carbon deposits was observed to have occurred in the original narrow regions where boron carbide had been obtained.

Although it is believed that leakage caused hydrolysis of the boron tribromide and a resulting lack of boron carbide formation, it had also been speculated (before discovery of the leak) that success in growing whiskers in the first run, and the lack of it in subsequent runs, was due to the use of a deposition tube and heating element used previously in the direct vapor process. These parts had therefore been exposed to the formation of nucleating species. Insertion of a similar piece of used graphite in a later run, in the deposition region, did not produce any deposit. However, this does not militate against the necessity for certain nucleating species, discussed in earlier reports concerning evaporative growth.^(1,2)

Successful growth of boron carbide whiskers, rather than blades, from mixtures of boron trihalide and a carbon vapor source in the preliminary runs made in a graphite furnace justify the conclusion that this process should be more efficient than the evaporative method. The whisker type X-ray pattern was similar, and the step like surfaces identify them as being of the same type as the evaporative process material.

In future studies, efforts will be made to broaden the area of deposition by altering concentrations and gas flow velocities, by exploring the temperature region around 1400°C, and by using various nucleating methods which have been in the past associated with the most efficient production of whiskers.

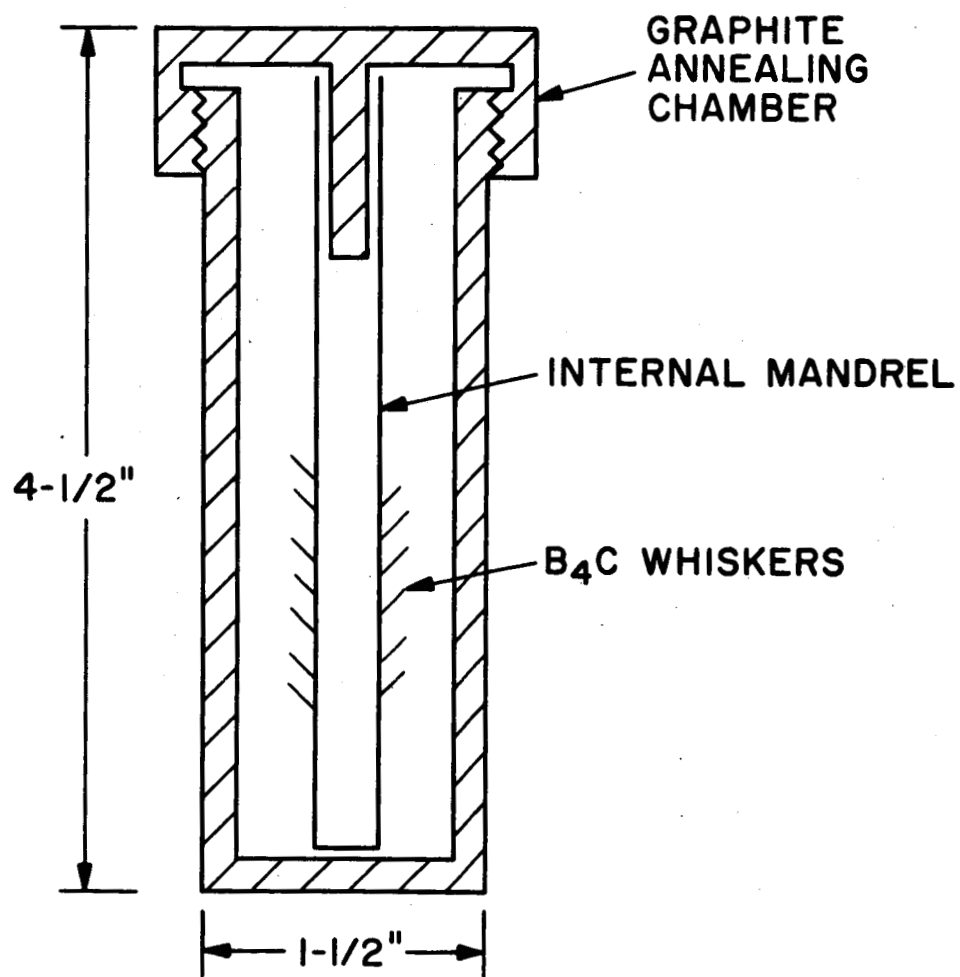
B. WHISKER ANNEALING STUDIES

Many of the B_4C whiskers grown by the direct vapor method were curved and also had growth steps on their surface. Curved whiskers have been shown to contain significant residual strains which decrease their potential strength. These residual strains will be discussed in the next section of the report.

Most whiskers which contained severe growth steps were weakened significantly because these growth steps acted as stress raisers with notch concentrations of 5 to 10. Previous results⁽²⁾ had shown that such areas undergo a change in geometry after extensive annealing and therefore, additional experiments were performed to determine whether annealing improves the properties of B_4C whiskers.

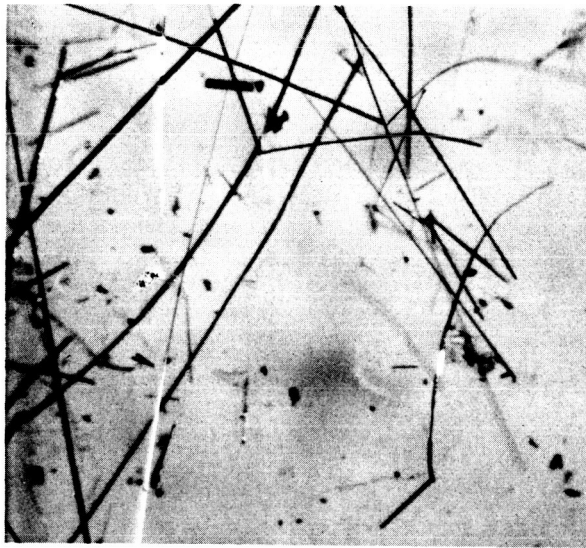
A graphite annealing box was designed which held an internal growth mandrel in an upright position as shown in Figure 6. The box containing the internal mandrel was placed into the chimney furnace such that it was heated uniformly to $1900^{\circ}C$ in vacuum and was held at temperature for 5 hours. Examination of the whiskers after annealing showed that significant changes had indeed occurred. Whiskers were notably less curved, and appeared smoother. Figure 7A is a typical internal mandrel scraping before annealing which shows a preponderance of curved whiskers. Figure 7B is a scraping of whiskers after annealing which contains no curved whiskers at all. Figure 8 is a photomicrograph which shows the smooth surface of a typical annealed whisker. Comparison of this surface with previously examined as-grown surfaces appears to show a definite trend toward smoother surfaces. However, as will be shown later (Fig. 13) the (0k0) plane of the B_4C whiskers has roughened considerably and is easily detected at high magnification.

The tensile test results of whiskers after annealing at $1900^{\circ}C$ were low; hence the annealing studies were extended to include one hour anneals at $1800^{\circ}C$, $1700^{\circ}C$, $1500^{\circ}C$, $1300^{\circ}C$ and $1100^{\circ}C$. Further studies on the morphology and crystal structure of annealed whiskers were also made and are presented in another section of this report.

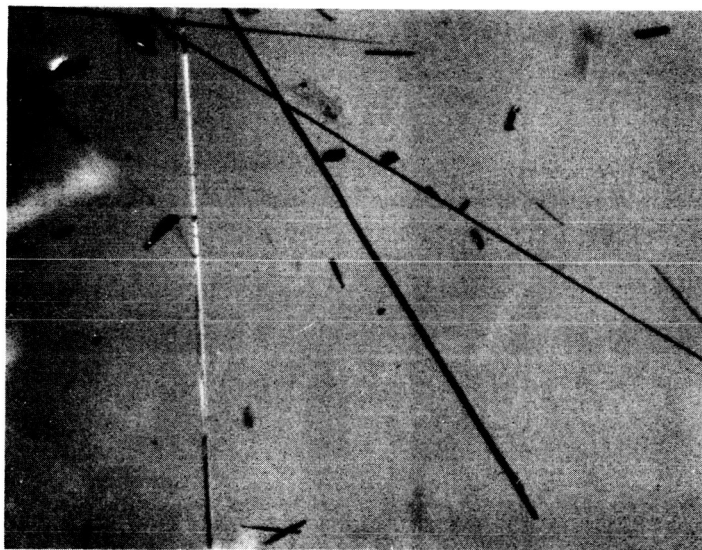


N 301-998A

Figure 6. Schematic Drawing of Graphite Chamber for Annealing B₄C Whiskers



A

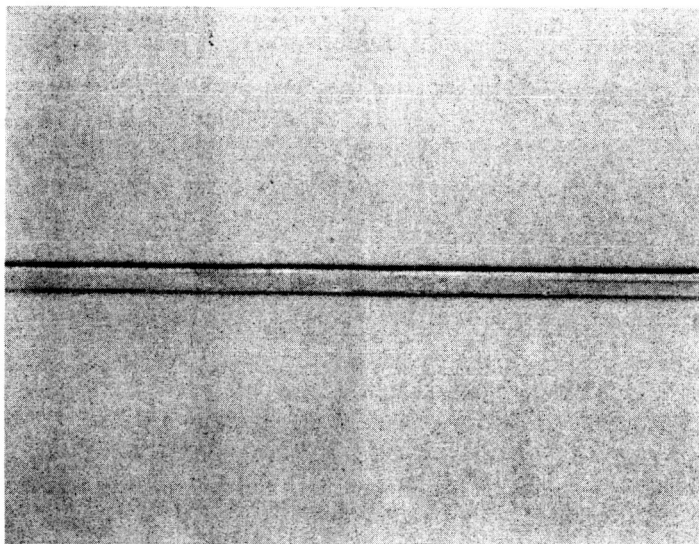


B

66-DI-173

Figure 7. Examples of Curved B_4C Whiskers as They Appear

- A) Before Annealing - (30X)
- B) After Annealing at $1900^{\circ}C$ for 5 hours - (30X)



66-DI-175

Figure 8. Example of Whisker Surface of An Annealed Whisker - 300X

The tensile data on all annealed samples (including previous work⁽²⁾) are presented in Table 1 and illustrated graphically in Figure 9. The results indicate that the strength of most whiskers is probably progressively reduced with increasing annealing temperature.

TABLE I
STRENGTH OF ANNEALED AND AS-GROWN B₄C WHISKERS

Spec. No.	Heat Treat	LT(mm)*	LO(mm)**	Area (μ^2)	σ m(psi)
1	1900°C 1 hr	1.50	0.60	92.6	100,000
2	1900°C 1 hr	1.84	0.55	43.5	336,000
3	1900°C 1 hr	2.90	0.77	43.6	147,000
4	1900°C 1 hr	4.24	0.57	71.5	169,000
5	1700°C 1 hr	---	1.71	38.8	184,000
6	1700°C 1 hr	4.53	0.86	163.0	272,000
7	1700°C 1 hr	5.57	1.98	31.5	326,000
8	1600°C 1 hr	3.32	0.54	5.95	1,200,000
9	1600°C 1 hr	2.60	0.44	68.0	370,000
10	1500°C 1 hr	3.89	0.49	21.8	490,000
11	1500°C 1 hr	3.59	0.58	264.0	324,000
12	1500°C 1 hr	3.77	0.55	9.4	295,000
13	1300°C 1 hr	3.38	0.66	11.5	566,000
14	1300°C 1 hr	2.87	0.60	24.1	710,000
15	1100°C 1 hr	2.28	0.50	30.5	410,000
16	1100°C 1 hr	4.95	0.46	42.5	735,000
17	as-grown	---	0.87	141.3	873,000
18	as-grown	4.51	0.35	22.4	760,000

* LT = Whisker Length

** LO = Test Gauge Length

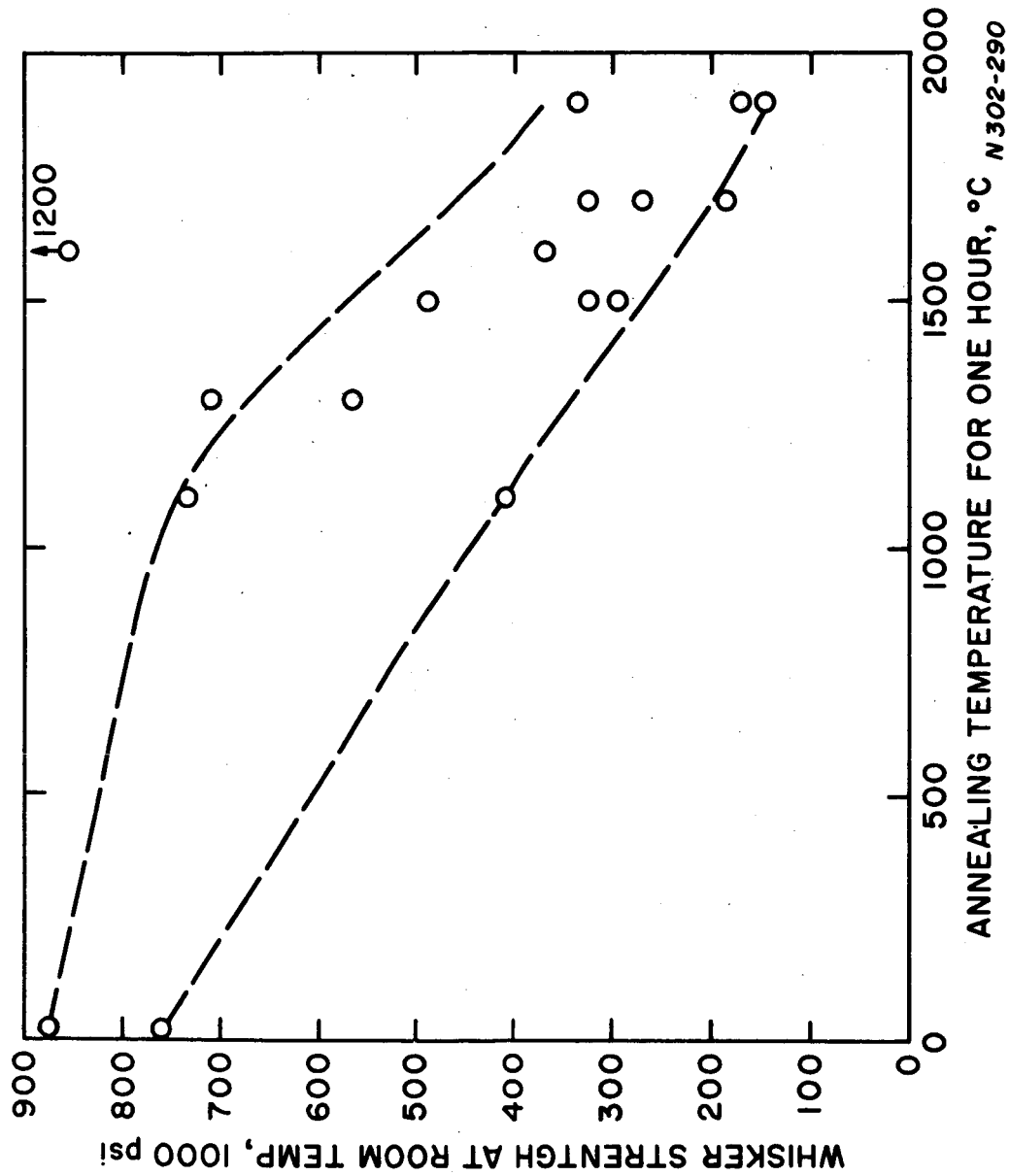


Figure 9. The Effect of Annealing Temperature on the Room Temperature Tensile Strength of B₄C Whiskers

C. WHISKER CHARACTERIZATION

1. Evaluation of Curved Whiskers

It had been observed that severely curved B_4C whiskers could not survive even slight manipulation and usually shattered in the region of high curvature. It appeared that this type of whisker probably contained internal residual strains. Therefore, an x-ray diffraction analysis was carried out to elucidate the internal strain character of curved B_4C whiskers. It was planned that precision lattice parameters a_o and c_o (hexagonal unit cell edges) would be obtained from the curved and straight portions of individual whiskers. If indeed there exist internal strains they would probably be detectable through measured differences in the magnitude of lattice parameters of the curved and the straight portions of the same whisker. In this way the magnitude and sign (compression or tension) of strains may be determined. A complete analysis was performed on only one curved B_4C whisker.

The hexagonal unit cell parameters, a_o and c_o , were determined from interplanar separation measurements, $d_{(hh0)}$ and $d_{(00l)}$, respectively. A General Electric single crystal orienter mounted on a G. E. XRD-5 diffractometer and nickel filtered copper radiation was used. The curved B_4C whisker was cemented to the end of a 1/10 mm diameter glass filament with Duco cement. After careful alignment, d_{110} , d_{220} , d_{330} and d_{003} , d_{006} , d_{009} , $d_{00.12}$, $d_{00.15}$ were determined for both the curved and straight portions of the whisker. The lattice parameters were then calculated from the hexagonal unit cell relationship:

$$\frac{1}{d_{(hkl)}^2} = \frac{4}{3} \left(\frac{h^2 + hk + k^2}{a^2} \right) + \frac{l^2}{c^2} \quad (4)$$

For the two types of interplanar spacings, namely $d_{(hh0)}$ and $d_{(00l)}$, the above relation can be written

$$a = 2h d_{(hh0)} \quad (5)$$

$$c = l d_{(00l)} \quad (6)$$

The experimentally determined d-spacings and the corresponding a and c values are given in Table II.

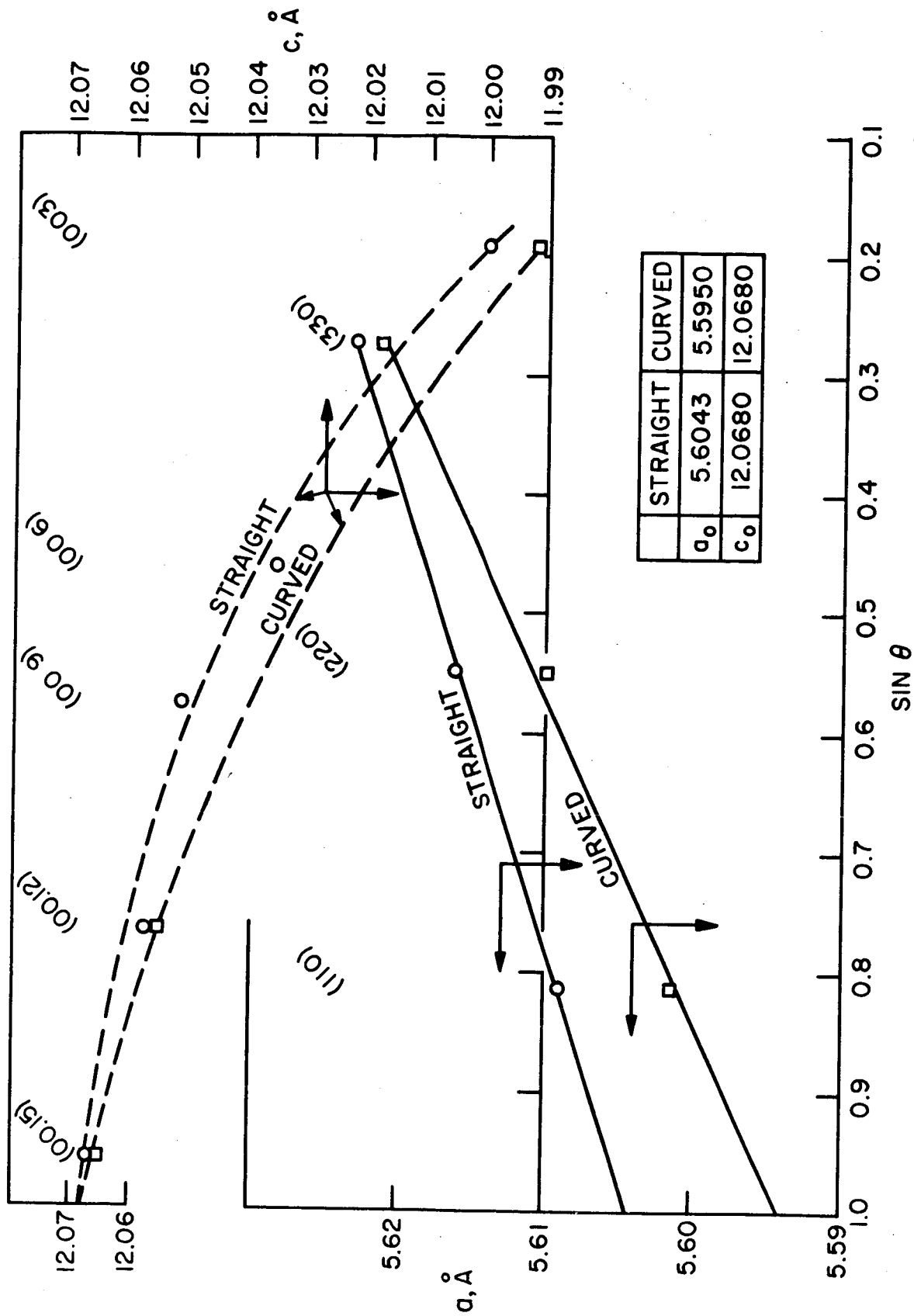
TABLE II
EXPERIMENTAL INTERPLANAR SPACINGS, d, AND CALCULATED
LATTICE PARAMETERS a AND c

hkl	Straight Section		Curved Section	
	d(\AA)	a(\AA)	d(\AA)	a(\AA)
110	2.8115	5.6230	2.8098	5.6196
220	1.4041	5.6164	1.4025	5.6100
330	0.93464	5.6078	0.93361	5.6017
	d(\AA)	c(\AA)	d(\AA)	c(\AA)
003	4.0012	12.0036	3.9973	11.9919
006	2.0060	12.0360	----	----
009	1.3391	12.0519	----	----
00.12	1.0048	12.0576	1.0046	12.0552
00.15	0.80448	12.067	0.80437	12.0655

Values for a_0 and c_0 were obtained by calculating $\sin \theta$ from the data in Table II and extrapolating to $\sin \theta$ equal to one ($\theta = 90^\circ$), as illustrated in Figure 10.

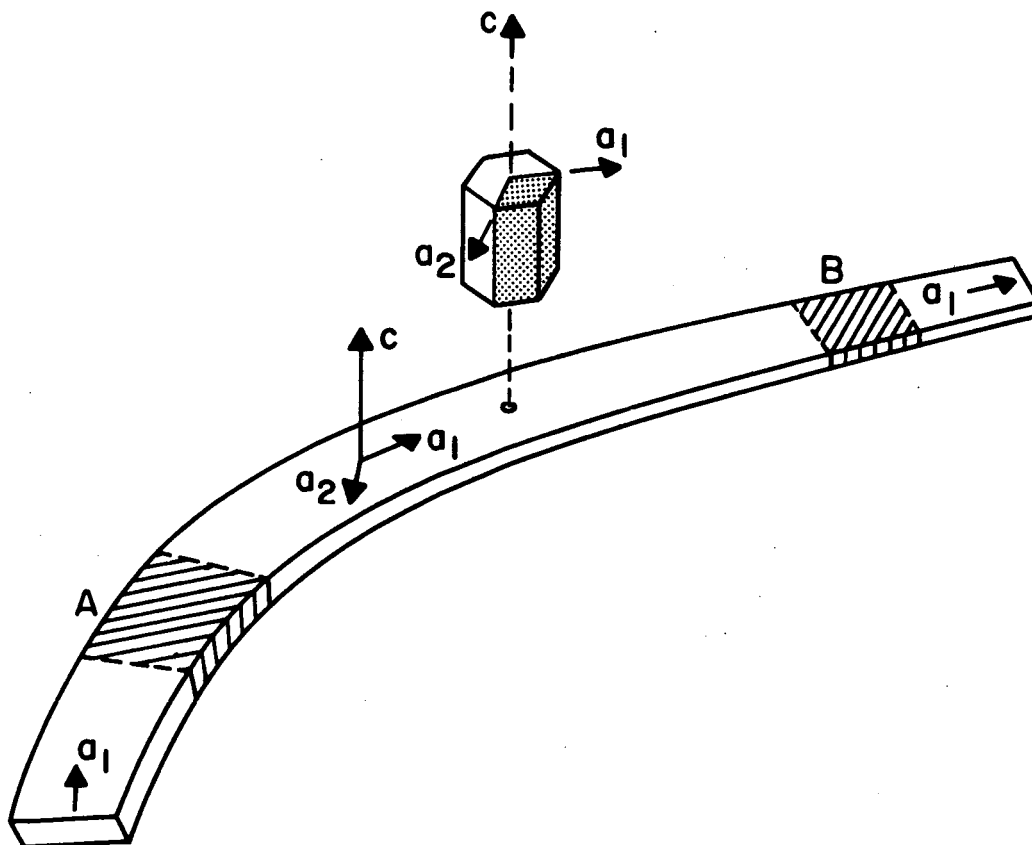
Figure 11 shows a sketch of the whisker used in this investigation. The curved major axis of this whisker, like all of its straight counterparts, was found to be everywhere parallel to the \vec{a} crystallographic direction. Shown in Figure 11 are crossed-hatched portions A and B, which are the curved and straight portions respectively from which x-ray diffraction data were obtained. Also shown is the orientation of the whisker with respect to the hexagonal unit cell directions. From the data presented in Figure 10 it may be seen that the extrapolated interatomic separations in the c-direction (i.e., $\langle 00\ell \rangle$) are the same for both the straight and curved portions of the whisker. However, the interplanar separation in the a-direction shows a contraction in the curved portion.

The contraction of \vec{a} corresponds to a compressive strain in the curved portion of the whisker. Assuming that the straight portion of the



N 301-999

Figure 10. Hexagonal Unit Cell Lattice Parameters a_o and c_o for Curved and Straight Portions of a Single B_4C Whisker.



N 302-001A

Figure 11. Sketch of A Curved B_4C Whisker. Lattice Parameters (a and c) were Determined from Curved Section A and Straight Portion B ($a_o^A = 5.5950\text{\AA}$, $c_o^A = 12.0680\text{\AA}$, $a_o^B = 5.6043\text{\AA}$, $c_o^B = 12.0680\text{\AA}$).

whisker is unstrained*, one may calculate the strain in the direction of curvature as follows:

$$\epsilon^{(curved)} = \frac{a_o^{(straight)} - a_o^{(curved)}}{a_o^{(straight)}}$$

$$\epsilon^{(curved)} = \frac{5.6043 - 5.5950}{5.6043}$$

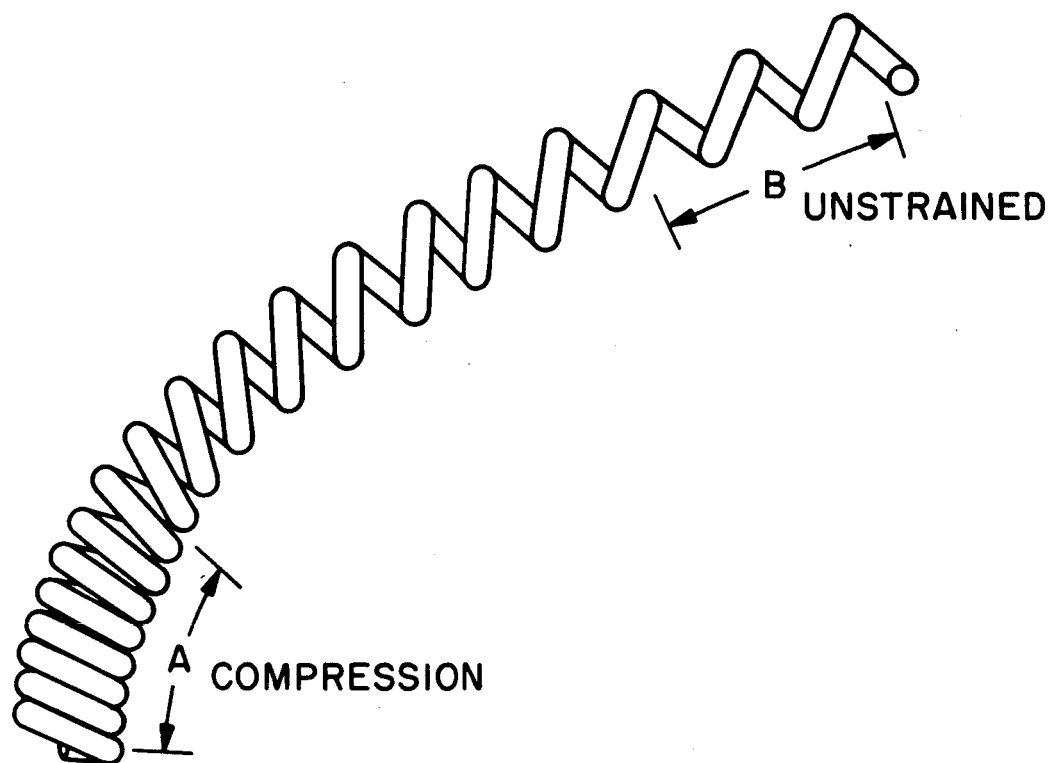
$$\epsilon^{(curved)} = 0.00166 \approx \frac{1}{600}$$

Thus, the internal stress σ^i in the curved portion of the whisker is (where E = modulus):

$$\begin{aligned}\sigma^i &= E \epsilon^{(curved)} \\ &= \frac{E}{600}\end{aligned}$$

Considering that the strongest whiskers (B_4C) tested to date have strengths in the order of 2×10^6 psi or $\frac{E}{30}$, the internal compressive stress is appreciable and may account for the observed weakness of severely curved whiskers. In Figure 12 is shown a spring analog of an internally stressed, curved B_4C whisker. The curved portion A is shown under compression while the straight region B is unstrained. This, of course, is not an equilibrium condition. The spring analog picture, based only on the resulting x-ray data, is incomplete. Naturally, a spring if strained in the manner shown in Figure 12 could not possibly be in equilibrium. What is needed even for pseudo-equilibrium are tension constraints in the curved portion of the whisker. It is believed that the tension constraints in the actual whiskers are very much localized, perhaps in a "thin-skin" surface region. If this were the case they would perhaps not contribute sufficiently to the diffracted x-ray intensity and thus (as was the case in this experiment)

*This assumption is not thought to be unreasonable since the lattice parameters obtained from the straight portion are in good agreement with ASTM values. Lattice parameters: straight portion ($a_o = 5.6043\text{\AA}$, $c_o = 12.068\text{\AA}$), ASTM values ($a_o = 5.61\text{\AA}$, $c_o = 12.07\text{\AA}$).



N 302-002

Figure 12. Spring Analog of Internal Stresses in a Curved B_4C Whisker. This Non-equilibrium Analog is Consistent with the X-ray Data of Figure 10

remain undetected. This reasoning explains the catastrophic failure when an attempt is made to handle or manipulate these curved whiskers.

2. Evaluation of Annealed Whiskers

Attempts were made to relieve internal whisker strains through thermal treatments and thereby strengthen the whiskers. This section describes the character of thermally treated whiskers, and explains why thermal treatment, although found to straighten the curved whiskers tends to weaken most of them.

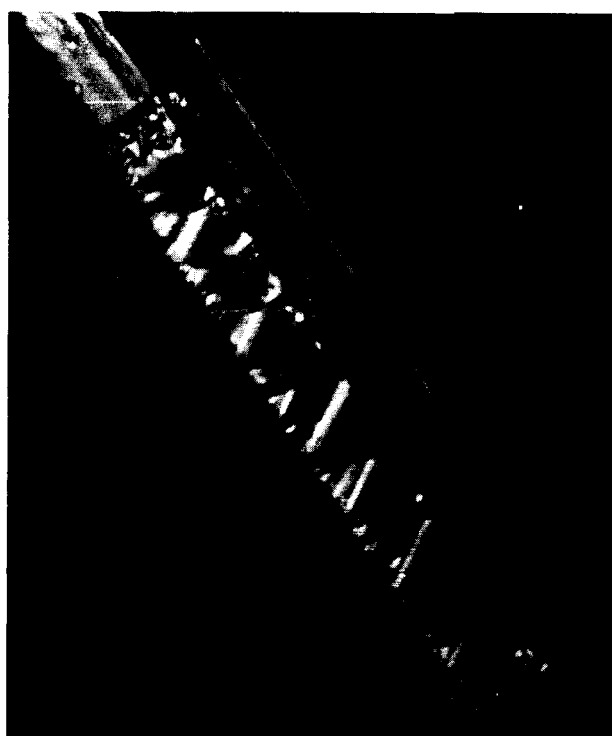
The effects to be described resulted when B_4C whiskers were thermally treated in a medium vacuum (.085 torr) for one hour at $1800^{\circ}C$. Figures 13A and 13B are photomicrographs of B_4C whiskers before and after thermal treatment respectively. X-ray diffraction analyses of the "before" and "after" specimens showed that they were B_4C single crystals. The whisker axis was parallel to the \vec{a}_1 hexagonal unit cell edge, i.e. $\langle h00 \rangle$ direction. There was no indication in the diffraction photographs of annealed whiskers that any new phases, e.g. oxides, nitrides, etc., had formed as a result of the thermal treatment. However, the diffraction method used in these studies would not, under normal conditions, be sensitive enough to detect "new" phases if their concentrations were below about one volume percent. Although most of the B_4C whiskers grown recently contain extensive smooth regions, the fields in Figure 13 show whisker regions in which typical steps are contained. These regions were chosen in order to illustrate the points which will now be discussed.

The major differences found between as-grown and annealed whiskers, other than the fact that heat treatment straightened the curved whiskers, were that the height of whisker steps on the $(00\bar{l})$ surfaces seemed to be reduced and more important, certain whisker surfaces, $(0k0)$, tended to become roughened. Typical roughening is illustrated in the left whisker edge shown in Figure 13B which can be compared with the as-grown whiskers shown in Figure 13A. In both cases the faceted surfaces are the $(00\bar{l})$ planes. Close examination of Figure 13B reveals that only those crystal surfaces parallel



A. BEFORE ANNEALING

10 μ



B. AFTER ANNEALING

Figure 13. B_4C Whiskers Before and After Annealing, $1800^{\circ}C$, 1 Hour, 85×10^{-3} Torr, Magnification = 1300X.

to the left edge experience roughening. The planes which intercept to form the surfaces in question are the (00ℓ) and $(0k0)$ planes. The (00ℓ) family of planes are parallel to the surface containing the triangular steps (e.g., parallel to the plane of the photograph) in Figure 13B. The $(0k0)$ planes are perpendicular to the photograph. A schematic representation of a portion of a typical annealed whisker showing the resulting roughening is given in Figure 14.

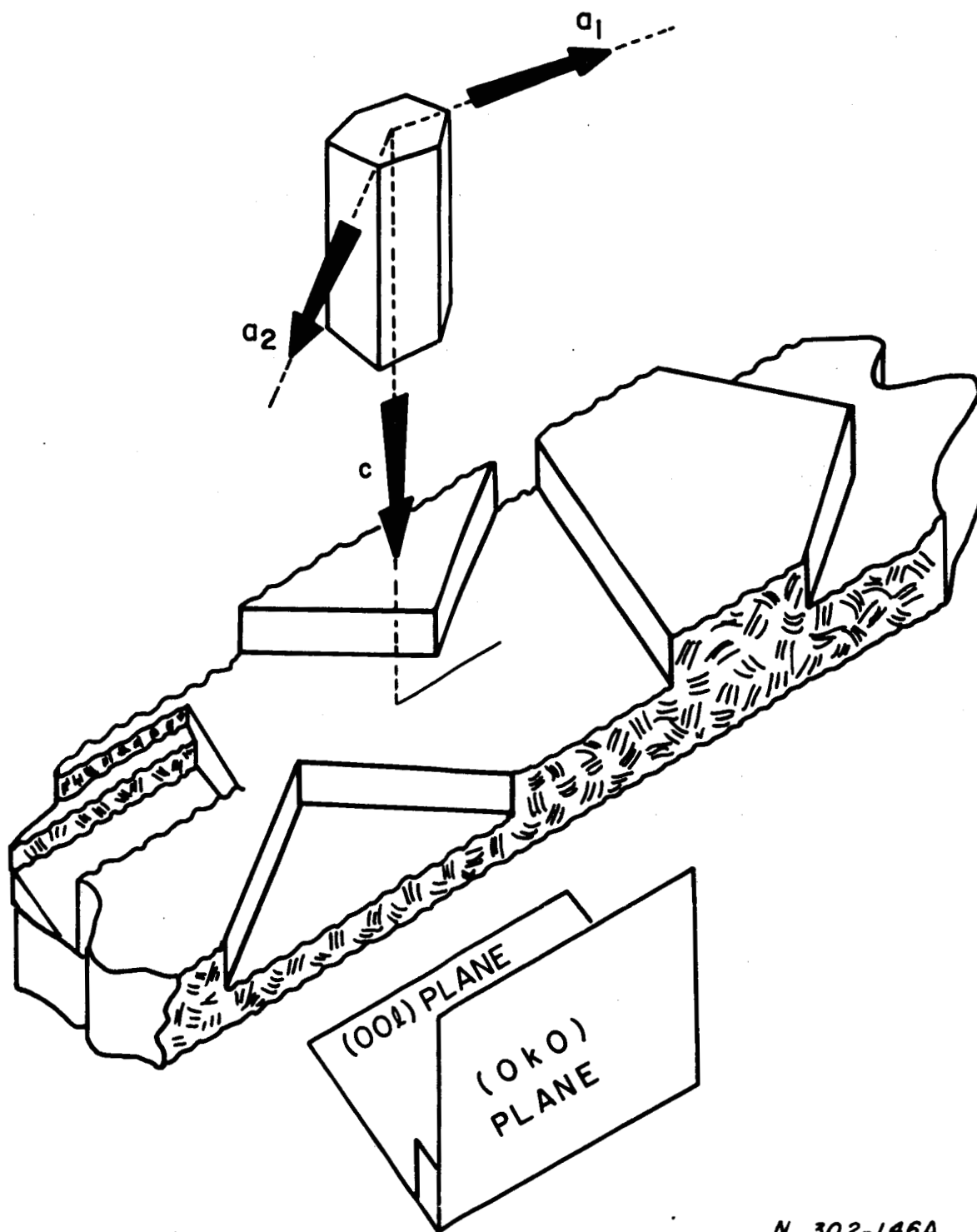
Roughening may result from one or both of the following reasons:

(a) The rate of evaporation of B_4C from the $(0k0)$ planes is markedly greater than from other planes. However, this does not seem to be likely since the overall appearance of the (00ℓ) planes are somewhat smoother after thermal treatment.

(b) The (00ℓ) plane edges are very reactive to the ambient atmosphere (air at 0.085 torr) during the annealing treatment of one hour at 1800°C . This appears to be the most logical explanation for the observed roughening.

As may be seen in Figure 13B, and is also shown in the sketch of Figure 14, the boundary or edge formed by a smooth (00ℓ) plane and a roughened $(0k0)$ plane is extremely irregular. Irregularities of this kind are in effect notches in the crystal. These notches act as stress raisers which weaken the crystal. Hence any gain in strength resulting from internal stress relief through straightening the whisker by annealing is probably more than offset by the weakening due to notch formation during the annealing process.

Therefore, unless annealing is done at low temperatures or at low pressures (ca. 10^{-6} to 10^{-7} torr) or in an inert atmosphere (e.g. He), annealing will probably be deleterious to whisker strength, as found in this work.



N 302-146A

Figure 14. Schematic Representation of Annealed B_4C Whisker Showing Roughened $(0k0)$ Planes and Resulting Edge Notches

III. COMPOSITE STUDIES

A. ALUMINUM-B₄C WHISKER COMPOSITES

Aluminum - B₄C whisker composites were fabricated by a liquid infiltration method developed earlier⁽²⁾. Before infiltration all whiskers were coated by a sputtering process with a duplex layer of nickel over titanium to promote wetting. After this the whiskers were separated into four groups, according to length, by screening. The long group of whiskers were at least 1/4" in length. The medium length group was in the 3/16" to 1/8" length range and the fine group was in the 1/8" to 1/16" range. A fourth group contained all the debris which was left.

The composites appeared to be of excellent quality, although, as has been the case in the past⁽²⁾, high volume fraction loadings of the specimens could not be achieved, because of difficulty in packing together curved whiskers with rough surfaces. Thus the tensile values obtained on the specimens (Table III) are only indicative of composites containing volume fractions in the 5 to 10 percent range as confirmed by cross-section studies of the fractured areas of the tensile tested specimens.

TABLE III
TENSILE DATA FOR B₄C-Al FORMED BY INFILTRATION TECHNIQUE*

Sample	Whisker Length, inches	UTS psi
080201		
Test #1 }		8,900
Test #2 }	> .25	9,400
080202		
Test #1 }		11,500
Test #2 }	.12 to .17	13,000
080203	.07 to .12	10,000

* All tests were performed at room temperature

$$\sigma_c = V_f \bar{\sigma}_f \left(1 - \frac{L_c}{2L_f} \right) + (\text{matrix contribution}) \quad (3)$$

Where:

σ_c = strength of the composite

V_f = volume fraction of the fibers in a composite

L_f = length of the fibers.

The matrix contribution is in many cases (i. e., for pure ductile metals) so small as to be negligible; however, it is readily calculable.

By combining equations (2) and (3) it is apparent that to obtain 95% of the available strength of any fiber, the fiber length must be at least 10 times L_c . At elevated temperatures, it can be expected that τ will decrease thereby increasing L_c ; hence even larger fiber lengths will be required for reinforcement at elevated temperatures.

Assuming an average diameter of 10 microns for B_4C whiskers, an average strength per whisker of 500,000 psi and a τ of 3,000 psi for aluminum at room temperature, then $L_c \approx .010$ inches.

Thus, it is apparent that whiskers of lengths longer than .1" are necessary before any appreciable strengthening of potential can be derived from B_4C whiskers.

It is also apparent then that the growth and separation of strong, smooth, straight, long B_4C whiskers still continues to be a critical problem area for study.

In order to experimentally determine values of L_c for B_4C fibers in aluminum, and to evaluate other critical factors, such as the interfacial bond strength and fiber-matrix wetting, which affect the transfer of stresses from the matrix to the fibers, a series of experiments were undertaken. These were based on using controlled lengths of B_4C/W filaments in aluminum.

B. ALUMINUM - B₄C/W FILAMENT COMPOSITES

The nature of most of the B₄C whiskers grown to date (i.e., their curvature, surface roughness, short length) has limited the present volume fraction of whiskers which can be incorporated into a composite. Also, the length of the whiskers must exceed a critical value to cause reinforcement of the matrix. The mechanical behavior of the composite materials made to date has thus not been studied in any great detail because of difficulties in physically evaluating the micro structural fractures of small whiskers, embedded in aluminum. It was felt that the substitution of continuous boron carbide filaments (produced by the vapor deposition of B₄C on a hot tungsten filament⁽³⁾ by the reaction $4\text{BCl}_3 + \text{CH}_4 + 4\text{H}_2 \rightarrow \text{B}_4\text{C} + 12\text{HCl}$ would fulfill the need for long, straight, strong B₄C filaments until such time as further study of the B₄C chemical vapor deposition process could produce acceptable whiskers. Also, the critical problems involved in the transfer of stresses from a ductile matrix to short, brittle fibers could be evaluated.

It has been also shown by Kelly⁽⁴⁾ and others⁽⁵⁾ that a critical length of reinforcing fiber is necessary before a transfer of stress from a matrix to a reinforcing fiber can occur. A rather simple relationship is derived by which an estimation of this critical length can be made, viz.:

$$L_c = \frac{\bar{\sigma}_f d_f}{2\tau} \quad (2)$$

Where:

L_c = critical length for reinforcement

$\bar{\sigma}_f$ = strength of fiber

d_f = fiber diameter

τ = shear strength of matrix (or interface)

Assuming that the rule of mixtures is valid, L_c then approximates the minimum length of fiber necessary to initiate any reinforcement.

Another derivation also attributable to Kelly⁽⁴⁾ is:

Accordingly, a supply of tungsten-core boron carbide filaments was chopped into two inch and 1/2" lengths and sputtered with a duplex Ni-Ti coating essentially duplicating the techniques for B_4C whisker preparation. The coated filaments were then bundled into 1/16" diameter graphite molds as a continuous parallel array, using the 2 inch long filaments and as a discontinuous parallel array, using the 1/2 inch long filaments. The bundles were infiltrated with molten aluminum. Two specimens of each type (continuous and discontinuous) were prepared. The tensile data and microstructural data derived from these specimens is given in Table IV. The average tensile strength of the B_4C/W fiber in the as-deposited condition was measured and found to be 215,000 psi. It can be seen that the composites reinforced with continuous filaments were essentially of theoretical strength. On the other hand, composites containing the discontinuous filaments were only about 70% of theoretical strength. Calculations of the critical length, L_c , for this material indicated that the reinforcing filaments 1/2" long were at least 5 to 10 times greater than L_c . Thus a predicted composite strength of 90% or better was expected. Such discrepancies as these are not yet well understood and are presently being studied in detail. It is possible that factors such as fiber misalignment play an important role. It is to be noted that many of the important geometric parameters associated with discontinuous array reinforcement were not controlled in these specimens presumably leading to large discontinuities in the structure which in turn contribute to premature failure. A summary of these factors attributable to Mehan and co-workers⁽⁸⁾ is shown in Figure 15.

In order to control the geometric parameters which are present in discontinuous reinforcing arrays, specimens were prepared by using hot pressing techniques. Figure 16 is a schematic diagram of this technique as it is presently being practiced.

A series of coated tungsten-core B_4C filaments of various lengths was selected to study a particular geometric parameter. These filaments were first slid into fine aluminum tubing of the same length and the tubing was crimped slightly so that they would stay in place. The sheathed filaments

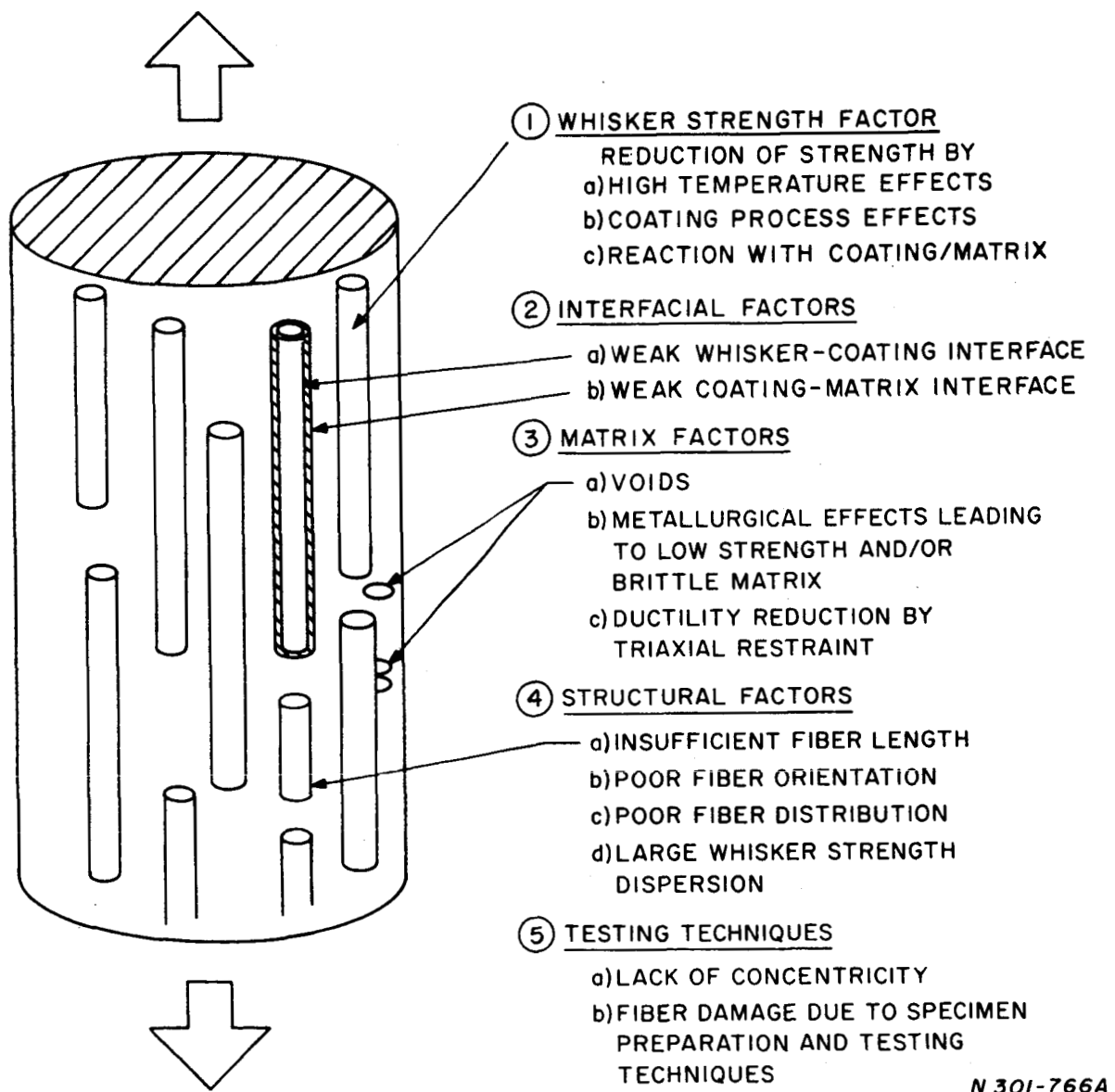
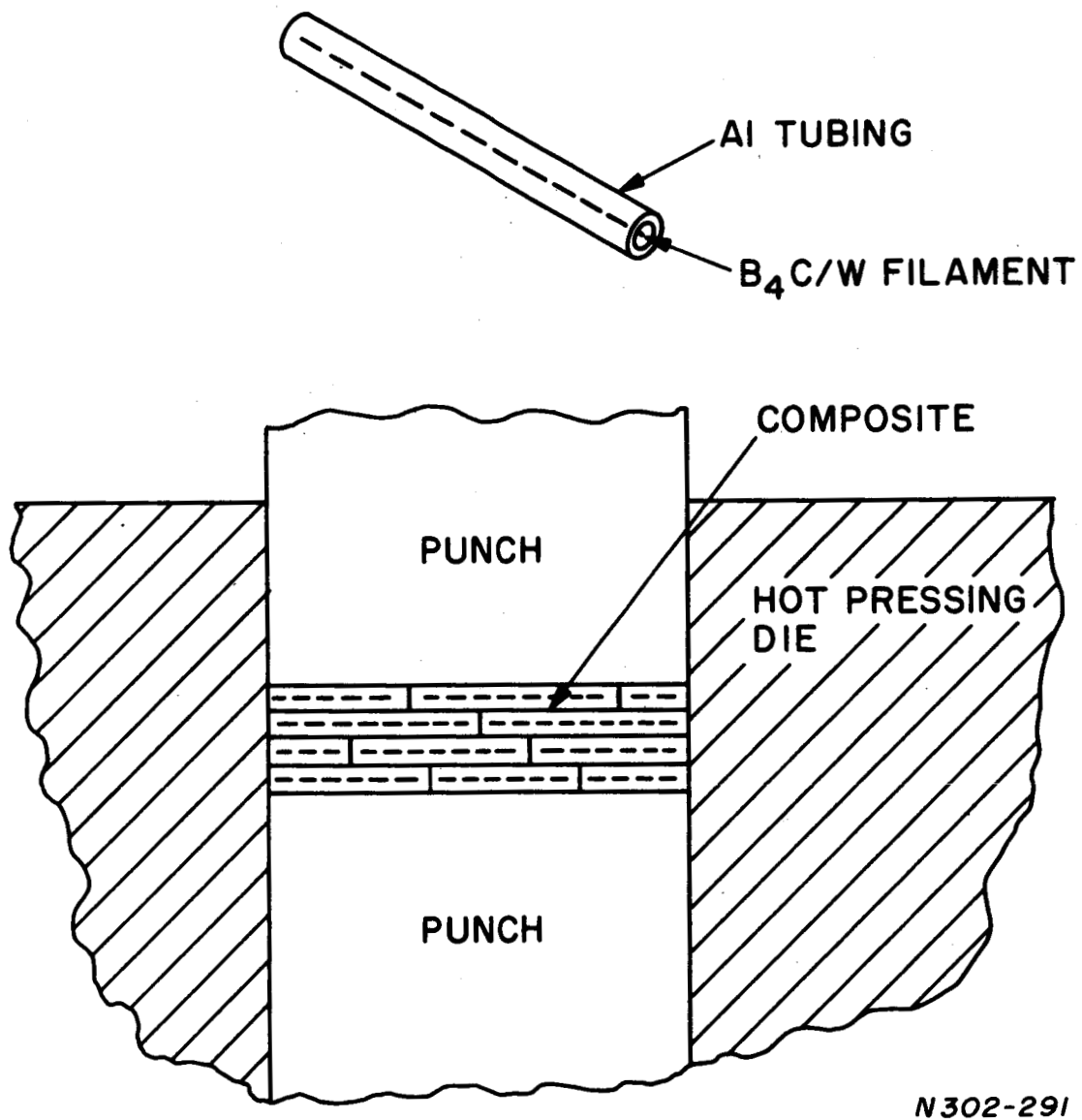


Figure 15. Resume of Possible Factors which Affect the Strength of Composite Materials Reinforced by Discontinuous Filaments (After Mehan and co-workers Ref. 8)



N302-291

Figure 16. Schematic Diagram Outlining the Hot Pressing Procedure for Producing B₄C/W-Aluminum Composites

TABLE IV
ROOM TEMPERATURE TENSILE PROPERTIES OF B₄C/W - ALUMINUM
COMPOSITES FORMED BY LIQUID INFILTRATION

Specimen #	Dia. (inches)	Breaking Load (lbs.)	Tensile Strength (1000 psi)	Number of Fibers per Cross Section Volume % Fibers	Stress Per Fiber 1000 psi	Percent of Theo- retical Reinforc- ing Fiber ⁽³⁾ Flow Stress
604051 ⁽¹⁾	.062	240	80	468/43.2	185	90%
604271 ⁽¹⁾	.051	175	86.2	295/40.0	215	100%
604272 ⁽²⁾	.047	107	61.7	249/40.5	152	71%
6042801 ⁽²⁾	.047	108	62.4	299/48.5	129	60%

(1) Continuous filament array

(2) Discontinuous Filament array

(3) Average fiber strength - 215×10^3 psi, fiber diameter .0019 inches.

were then placed into a pre-determined geometric array within the cavity of a hot pressing die. The die assembly was then brought to temperature and the array was hot pressed to a dense composite body.

Aluminum tubing is available ranging from 0.010" outside diameter with walls 0.002" thick and higher, so that various parameters such as distance between fibers can be varied and reasonably controlled. The electroplating of aluminum on filament and/or the coating of individual filaments by molten aluminum will be investigated in the near future. However, the aluminum tube approach is currently the simplest technique which introduces the fewest processing variables while still providing the specimens necessary for studying the mechanical behavior of B₄C reinforced composites.

The apparent value of L_c necessary to induce reinforcement in a composite is an important parameter, the study of which is the first step toward understanding the mechanical behavior of composites. A composite

containing less than a critical volume of reinforcing fibers, provides a method for estimating L_c because the matrix can flow plastically thereby breaking the bonded fibers into their respective apparent critical lengths.⁽⁴⁾ Accordingly, a number of aluminum specimens 4 inches long by approximately 1/8" x 1/8" each containing a single two-inch long B_4C/W filament within its geometric center were fabricated by the hot pressing technique discussed above. A sketch of the fabrication details and final specimen produced is shown in Figure 17.

Three such specimens were pulled in tension and then immersed in 50% HCl to dissolve the aluminum matrix. The broken pieces of filament were recovered in order to measure their lengths (i. e., apparent values of L_c) and to examine the fracture modes. Table V contains the pertinent length measurements, and Figure 18 illustrates the length and uniformity of several groups of filaments. Figure 19 shows representative fracture surfaces.

Specimen No. 1 failed in the grip during the first attempt at a tensile test. It was retested and failed in the gage length. The size of the broken pieces is identified separately in Table V for the two halves of the gage length. Specimens 2 and 3 also failed in the grip during the initial attempts to pull them in tension.* Their intact gage lengths were immersed in 50% HCl without any further attempts to break them. The difference in the results between specimens 2 and 3 (Table V) suggest that the different test procedure applied to specimen No. 1 had no significant effect on the lengths of the broken pieces of filaments. It seems probable that fabrication procedures control both the length and uniformity of the filament sections. Specimen No. 2 had the smallest and most uniform sections (see Fig. 18).

Many of the retrieved broken pieces of filament were examined and fracture modes typical of tensile failure in boron filaments⁽⁹⁾ were found. Fig. 19A shows a very smooth fracture of a type which originates

* 10-15% permanent uniform elongation in gage length, whereas the fracture strain of the B_4C/W filaments is less than 1%.

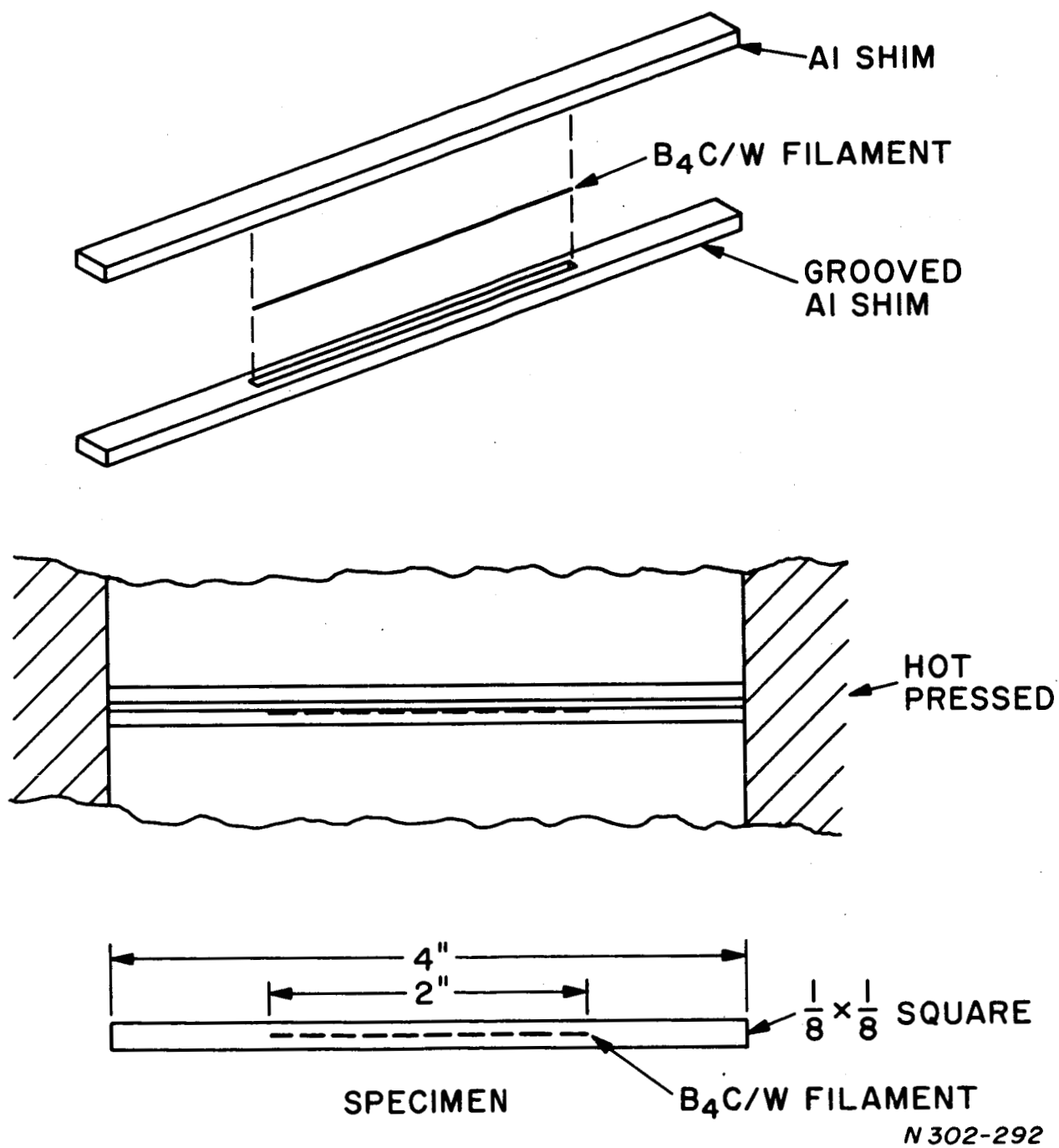
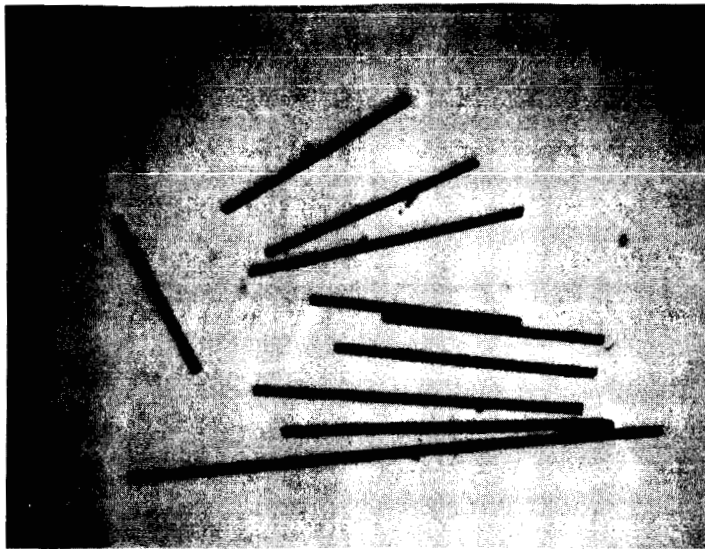
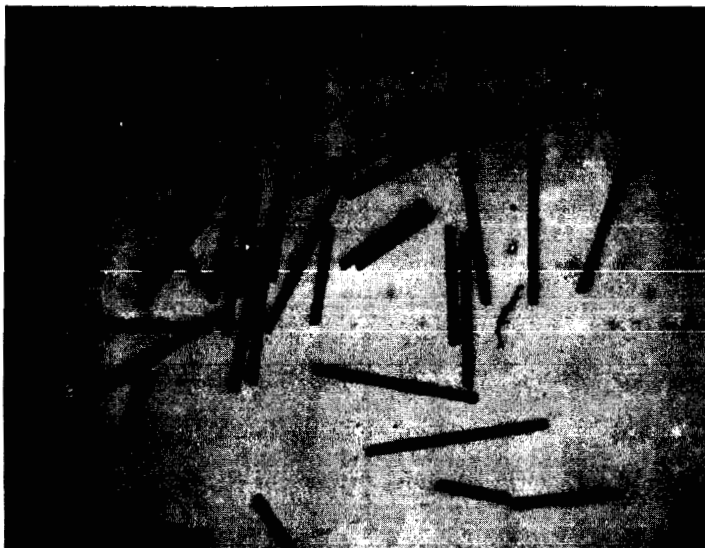


Figure 17. Sketch Showing Processing Details to Produce B_4C/W -Aluminum Composites for Estimating Values of the Filament Critical Length, L_c



(A) SPECIMEN NO. 1A

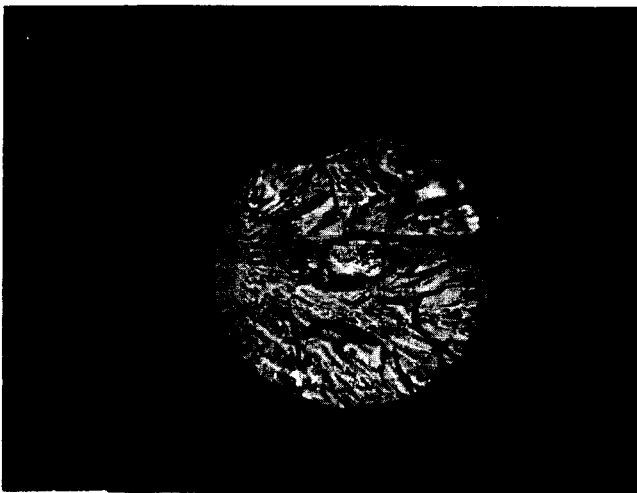


(B) SPECIMEN NO. 3

Figure 18. Broken Sections of B_4C/W Filaments Retrieved From Hot Pressed Aluminum Composites (17X)



(A) LOW-STRENGTH FAILURE
FILAMENT DIAMETER =
0.0027 INCH
 B_4C COATING THICKNESS =
0.00021 INCH



(B) INTERMEDIATE-STRENGTH
FAILURE



(C) HIGH-STRENGTH FAILURE

Figure 19. Typical Tensile Fractures of B_4C/W Filaments in Hot Pressed Aluminum Composites (593X)

TABLE V
THE DIMENSIONS OF BROKEN PIECES OF 2-INCH LONG B₄C/W
FILAMENTS RETRIEVED FROM HOT-PRESSED ALUMINUM
COMPOSITES AFTER TENSILE TESTING

Specimen No.	No. of Pieces Retrieved	Length-Inches (Min.) (Max.) (Avg.)	Remarks
1A	10	0.059 (0.165) 0.086	Approximately 75% of Filament in the Gage Length (see Fig. 1A)
1B	6	0.071 (0.288) 0.175	Approximately 25% of Filament in the Gage Length
1*	16	0.059 (0.288) 0.119	Combination of above (47.5% of Filament in Gage Length)
2	47	0.022 (0.059) 0.043	1.5-Inch of the Filament (87.5%) in the Gage Length (see Fig. 1B)
3	15	0.018 (0.208) 0.131	All of the Filament in the Gage Length

in the interior of the specimen and is invariably associated with low tensile strength (< 100,000 psi). This kind of failure was least common. More common was failure originating at the filament surface, as shown in Figure 19B. This kind of failure is ordinarily associated with intermediate tensile strengths. Figure 19C shows a "cone to cone" fracture which, while it originates at the core-sheath interface, is associated with the higher tensile strength levels (> 450,000 psi) in boron filaments. The fact that this was the most common type of failure suggests that the fabrication procedures are frequently good enough to exploit the high strengths characteristic of short filament lengths.

* Considered as a single specimen.

IV. DISCUSSIONS AND CONCLUSIONS

1. The growth of B_4C whisker has been studied by two methods, the evaporation of B_4C with subsequent condensation to form whiskers and the chemical vapor deposition process which uses gaseous species containing boron, carbon and hydrogen to subsequently form B_4C whiskers upon co-reaction. The chemical vapor deposition process is more amenable to scale-up because it can be operated at lower reaction temperatures than the direct vaporization process and the available B_4C forming gases which form whiskers are independently controlled by external means.

The direct evaporation whisker deposition area configuration has passed through a series of geometric changes in the search for an efficient method for growing long, straight nearly perfect B_4C whiskers. A deposition chimney with no internal mandrels was the first modification which grew B_4C whiskers successfully for the first time. An internal mandrel was later added to increase the surface deposition area and use the available volume of B_4C vapor more effectively. This internal mandrel addition increased the whisker growth rate by an order of magnitude. A third modification used a new approach. A graphite resistance furnace of radial geometry was modified so that its graphite radiation shield could be used as a deposition zone for B_4C whisker growth. Results of this modification reported in an earlier contract⁽²⁾ (NASw 1205) were encouraging in that the number of whiskers grown per run increased enormously and the whisker product was composed of straight B_4C whiskers. However, the whiskers were too short (less than .1" long) for effective reinforcement potential in composites. Further attempts to increase the length of these whiskers during the early portion of this reporting period failed. It became apparent that the length limit of B_4C whiskers which can be grown by this modification is a function of the furnace design which cannot be altered significantly. Finally a third change in the deposition geometry of the standard chimney type furnace has led to an order of magnitude increase in whisker yield per run over that obtained previously. The internal mandrel design was replaced by crossed

thin graphite plates. It is believed that this is an important contribution because it is the second time during the development of B_4C whisker technology that such an increase in yield has been achieved. The geometry change has also altered the temperature gradient situation within the deposition area so that more long and straight whiskers are being grown.

2. Although considerable progress has been made in B_4C whisker growth technology using the direct evaporation method, geometric conditions existing within the growth area restrict the perfection and ultimate length of whiskers which can be grown. Further, the evaporation process is not amenable for scale-up because of low material transport rate and high operating temperatures. Thus, a more exhaustive study of the chemical vapor deposition process been started. B_4C whiskers grown by this process appear to be identical to whiskers grown by the pure vapor method although grown at significantly lower temperatures.

3. X-Ray diffraction studies of a curved whisker has shown that residual stresses of the order of 100,000 psi are present in portions of the whisker. Such residual stresses are certainly not desirable and means must be found to avoid growing curved whiskers or to minimize the effects through annealing, etc.

4. Annealing studies have shown that extensive weakening of B_4C whiskers occurs when the whiskers are heated in vacuum for one hour at elevated temperatures. Although an apparent decrease in the (00 l) surface roughness and the curvature of as-grown whiskers occurs, annealing results in an excessive loss of material by evaporation or reaction (from the (0 k 0) surfaces) and has a weakening effect on the whiskers.

5. Thus far, composites of Al- B_4C whiskers have been prepared where the volume fraction of whiskers is low. To achieve high volume fractions, the whiskers should be smooth, straight, and long. Since the problems of surface roughness and curvature of B_4C whiskers grown by the direct vapor method have not as yet been solved, whisker packing densities have been limited to the range of 5 to 10 volume percent.

6. Composites using continuous tungsten-core B_4C filaments as a substitute material for B_4C whiskers were fabricated. Specimens containing continuous arrays of these filaments utilized essentially the full strengthening potential of the individual filaments. Discontinuous arrays however were only 70% effective rather than 90 to 95% effective as predicted by theory.

7. A hot pressing technique has been developed which permits fabrication of specimens containing pre-determined discontinuous arrays of filaments with reasonable precision. This technique was used to prepare specimens for studying the apparent critical length of the available continuous filaments. At present it is not possible to make a definitive quantitative statement concerning the critical fiber length, L_c , because the tensile strength of very short lengths of filament is unknown. The present results seem quite satisfactory for several reasons: a) the technique permits recovery and measurements of the broken sections b) reasonably good quantitative reproducibility is obtainable and most important, c) the fracture mode of the broken pieces indicates good utilization of the filament tensile strength.

REFERENCES

1. A. Gatti, R. Cree, E. Feingold, "Synthesis of Boron Carbide Filaments," NASw-670 Final Report, July 10, 1964.
2. A. Gatti, C. Mancuso, E. Feingold, R. Jakas, "Study of the Growth Parameters Involved in Synthesizing Boron Carbide Whiskers," NAWw-1205, Final Report March 1, 1966.
3. A. Gatti, J. B. Higgins, R. Cree, E. Feingold, "Boron Carbide Continuous Filaments," TR AFML - TR-65-354, Nov. 1965.
4. A. Kelly and G. J. Davies, "The Principles of Fibre Reinforcement of Metals," Met. Rev., 1965, Vol. 10, No. 37.
5. W. H. Sutton and J. Chorne', "Potential of Oxide-Fiber Reinforced Metals," Fiber Composite Materials, ASM 1964.
6. A. Gatti, C. Mancuso, E. Feingold, R. Mehan, R. Cree, "Study of the Growth Parameters Involved in Synthesizing Boron Carbide Filaments," NASA CR-251, July 1965.
7. K. M. Merz, "Silicon Carbide" Ed. J. R. O'Connor and J. Smittens, Pergamon Press, p. 78, 1960.
8. R. L. Mehan, C. A. Bruch, E. Feingold, to be published.
9. J. M. Berry, Task 6, "Research on Improved High-Modulus, High Strength Filaments and Composites thereof." Sept. 1965, General Electric Company, U.S.A.F. Contract AF 33(615) - 2126 Technical Report AFML TR-65-319.

ACKNOWLEDGEMENTS

Acknowledgement is given to Messers. T. Harris, R. Grosso, J. Lazur for their valuable assistance in this program and to Drs. W. H. Sutton and C. A. Bruch who reviewed the manuscript.